The quest for specialist N_2O-respiring bacteria

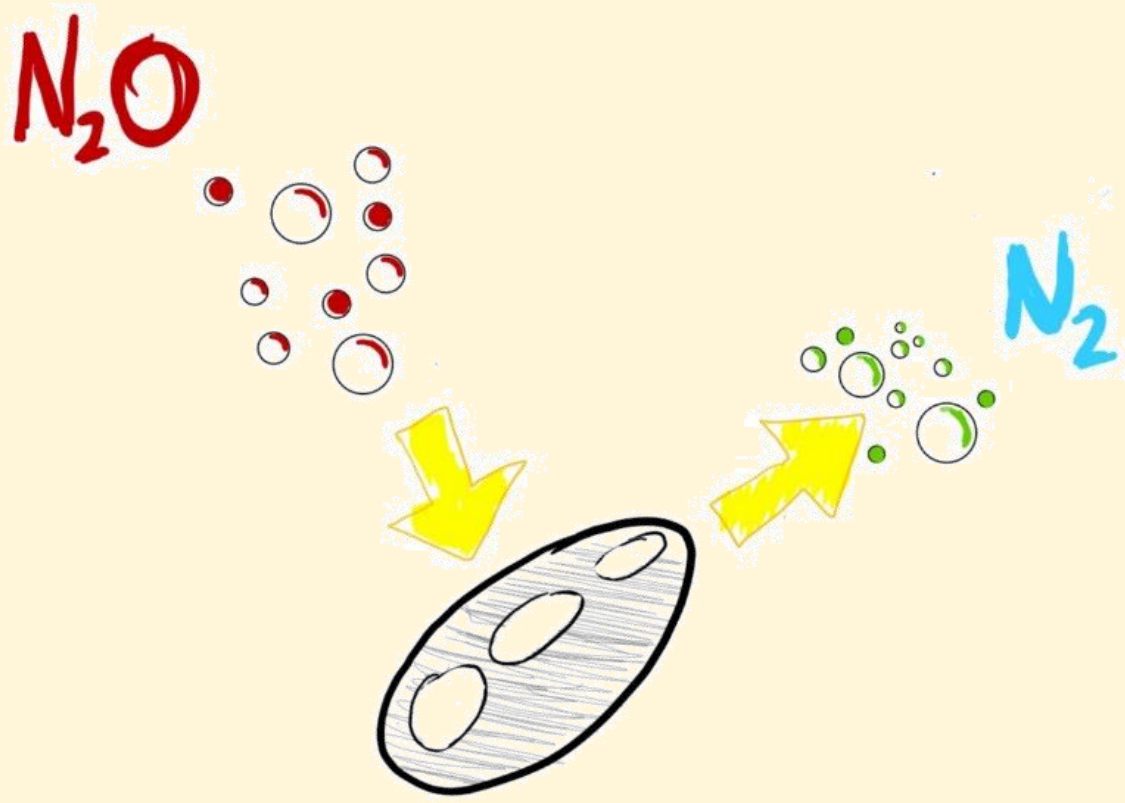

TU Delft

Francesc Corbera Rubio

The quest for specialist N_2O-respiring bacteria

Master Thesis

21/05/2019

Francesc Corbera Rubio

Student no.: 4747526

in partial fulfilment of the requirements for the degree of

Master of Science
in Life Science & Technology

at the Delft University of Technology

to be defended on 28/05/2019 at 16:00h.

Responsible thesis supervisor: Mark van Loosdrecht, Full Professor
Daily supervisor: Michele Laureni, Postdoctoral Researcher

Committee member: Mark van Loosdrecht, Full Professor
Committee member: David Weissbrodt, Assistant Professor
Committee member: Ludovic Jourdin, Assistant Professor

conducted at the:

Environmental Biotechnology Section, Department of Biotechnology, Faculty of Applied Sciences
Delft University of Technology, van der Maasweg 9, 2629 HZ Delft, The Netherlands

Correspondence: f.corberarubio@student.tudelft.nl; m.laureni@tudelft.nl

ABSTRACT

Nitrous oxide (N_2O) is a potent greenhouse gas, and its stratospheric concentration is already 20% above the pre-industrial level. Over 70% of N_2O is produced by microbial processes. Nitrous oxide reductase is the only enzyme able to reduce N_2O to innocuous N_2. The high abundance of organisms harbouring it and lacking the genetic potential to produce N_2O, commonly known as specialist N_2O-reducers, has only been recently disclosed in diverse ecosystems. In this work, we aim to understand which mechanisms select for them in open cultures and how N_2O affects cellular metabolism. Two continuously-fed stirred-tank membrane reactors (CSTMR) were run at 20 °C, pH 7 and low dilution rate (0.14 d^{-1}) under either acetate- or N_2O-limiting conditions. Denitrifying activity could not be completely washed out from the reactors. Yet, a ten orders of magnitude increase in clade II *nosZ* gene abundance, often associated with specialists, was found under N_2O limitation. Moreover, cultivation under N_2O excess resulted in 30-50% lower biomass yields and a 25% higher maintenance coefficient as compared to N_2O limitation. Lastly, polyhydroxyalkanoates (PHA) consistently accumulated (up to 20 wt%) under both acetate and N_2O limitation, and the possible biochemical mechanisms are discussed. We conclude that *(i)* affinity for N_2O was not selective enough to enrich for specialist N_2O-reducers under the imposed conditions, and *(ii)* provide further evidence for the potential cytotoxicity of N_2O on the cellular metabolism and, to the best of our knowledge, *(iii)* report the first evidence of PHA accumulation in N_2O-respiring enrichments.

ACKNOWLEDGEMENTS

To Michele, whose supervision was outstanding in every sense. My most sincere thanks for sharing your knowledge and your enthusiasm. And for caring so much.

To Mark, who allowed me to work in EBT. And again to him, Robbert, Dimitry and Monica for their wise advise and contribution.

To EBT and TU Delft. For the opportunity to grow so much. Scientific and personal wise. Specially to Nina, my very good friend and N_2O mate, and David Weissbrodt, who kindly adopted me in his group.

To my friends, both LST and flatmates. You made my time here amazing. Marc, Miguel, Ainhoa, Queralt, Panos, Lolo, Britt, Fernando, Sara…

Special thanks to Sergio and Maxim. My strongest support. Delft feels like home because of you.

Y, sobre todo, a mi madre, al meu pare i al meu germà.

CONTENTS

1. INTRODUCTION

Nitrous oxide (N_2O) is one of the main contributors to the greenhouse effect (Muñoz et al. 2010) (Muñoz et al. 2010) . Its global warming potential has been estimated to be around 300 times higher than that of CO_2, which results in N_2O contributing to 5-9% of the anthropogenic emissions (3100 $TgCO_2$-eq yr^{-1}), yet accounting for only 0.03% of the total gas emissions (4-12 TgN yr^{-1})(Montzka et al. 2011; Thomson et al. 2012). Additionally, N_2O plays a major role in the ozone layer depletion. Once released to the stratosphere it can be converted to nitric oxide (NO), which promotes the depletion of ozone (Portmann et al. 2012; Ravishankara et al. 2009). Consequently, despite its low atmospheric concentration (332 ppb), N_2O has recently been catalogued as one of the main contributors to climate change (IPCC 2014)(IPCC 2014) due to the rise in its emissions (Machida et al. 1995), long lifetime (Hsu et al. 2010; Prather et al. 2015) and large environmental impact (Ravishankara et al. 2009).

A steady increase in the atmospheric N_2O concentration of 0.8 ppb·yr^{-1} was registered between 1979 and 2005 (Hall et al. 2007; Saikawa et al. 2014) and attributed to the uprising use of nitrogen fertilizers in response to increasing food demand (Muñoz et al. 2010; Thomson et al. 2012). Since demand is only expected to increase (Tilman et al. 2011), mitigation strategies of the N_2O emissions are urgently needed.

Multiple reactions produce N_2O, yet only one consumes it

Multiple sources of nitrous oxide are known, with the dominant ones being bacterial denitrification and ammonia oxidation (Figure 1) (Kool et al. 2011; Schreiber et al. 2012). The impact of the abiotic processes is relevant (Soler-Jofra et al. 2016; Wrage et al. 2001), albeit less than that of the biotic ones. Overall, microbial conversions alone account for 70% of the global N_2O emissions (Braker et al. 2011; Thomson et al. 2012). On the contrary, there is only one known biological N_2O sink: its reduction to dinitrogen gas (N_2), catalysed by the nitrous oxide reductase (nosZ) (Jones et al. 2013).

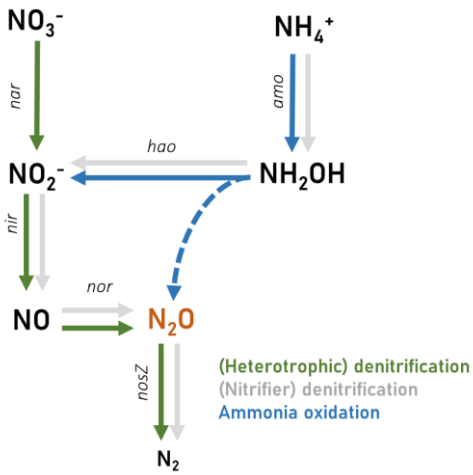

*Figure 1. Main sources of nitrous oxide emissions. Bacterial denitrification can occur in form of **heterotrophic denitrification**, carried by denitrifiers, or as **nitrifier denitrification** by nitrifiers. In the first one, nitrate (NO_3^-) is reduced to nitrite (NO_2^-), nitric oxide (NO), N_2O and dinitrogen gas (N_2) by enzymes nar, nir, nor and nosZ, respectively In the latter, the oxidation of ammonia (NH_4^+) to nitrite is followed by the reduction of this compound to $N_2(O)$. Nitrous oxide is produced during **ammonia oxidation** as well. Hydroxylamine (NH_2OH) is reduced by hydroxylamine reductase (hao) to NO, which is then reduced to N_2O by a yet unidentified nor. The first part of this reaction is not depicted for simplicity.*

Specialists N_2O reducers act as natural sinks

Microorganisms that can reduce nitrous oxide to dinitrogen gas can be divided in *i.* non-denitrifying N_2O reducers, which can remove nitrous oxide but not produce it (specialists), acting as net N_2O sinks; and *ii.* denitrifying N_2O reducers, which both consume and produce N_2O (generalists) (Jones, Spor, Brennan, Breuil, Bru, Lemanceau, Gri, et al. 2014).

Recent studies have described the existence of a new nitrous oxide reductase (*nosZ* II), sharing less than 50% of the amino acids with the canonical one (*nosZ* I) found in alpha, beta and gammaproteobacteria (Hallin et al. 2018; Sanford et al. 2012). This phylogenetic difference has led to the classification of N_2O reducers in two different clades. Approximately 83% of clade I nosZ bacteria contain the whole denitrification pathway (generalists), while 51% of clade II nosZ appear to be non-denitrifying N_2O-reducers (specialists) (Graf et al. 2014). The ratio and abundance of the two clades (I:II) have been proved to positively correlate with the ratio of N_2O/N_2 emissions in agricultural soils (Domeignoz-Horta et al. 2015, 2016; Jones, Spor, Brennan, Breuil, Bru, Lemanceau, Gri, et al. 2014). Consequently, clade II nosZ presence seems to be a good indicator of the abundance of specialists N_2O-reducers, which are a key factor to mitigate N_2O emissions.

Are specialists N_2O reducers slow growers?

Interestingly, isolated strains of clade II nosZ microorganisms have reported higher N_2O affinity and growth yields when compared to clade I nosZ (Yoon et al. 2016), probably due differences in the electron transport chain (Conthe, Wittorf, Kuenen, Kleerebezem, Hallin, et al. 2018). Lower maximum growth rates were found as well. In fact, there is an extensive body of literature proving that *nosZ* II organisms are more abundant than *nosZ* I in certain soils, where N_2O concentrations are low (< 5 ppm)(Metay et al. 2007; Yanai et al. 2011) and slow-growing organisms are not washed out due to their ability to form biofilms (Jones et al. 2013; Orellana et al. 2014).

To date, the only long-term studies of bacterial growth based on N_2O-reducing capacity in an open culture have been carried by (Conthe, Kuenen, et al. 2018; Conthe, Parchen, et al. 2018; Conthe, Wittorf, Kuenen, Kleerebezem, Hallin, et al. 2018; Conthe, Wittorf, Kuenen, Kleerebezem, Van Loosdrecht, et al. 2018). Neither higher affinity nor higher growth yields were identified in clade II nosZ species compared to nosZI under those conditions, contradicting previous research (Hallin et al. 2018; Yoon et al. 2016). However, fluctuations in the clade II abundance were found when the solids retention time (SRT) varied, even slightly. Specifically, a 100-fold increase with a 4-fold rise in the SRT was reported, which correlated with the increment of the specialists:generalist ratio as well, based on functional genes quantification (Conthe, Wittorf, Kuenen, Kleerebezem, Van Loosdrecht, et al. 2018).

All these findings lead to the hypothesis that specialists N_2O-reducers might have lower maximum growth rates than the generalists. Therefore, the retention times commonly imposed might have hampered their enrichment, masking their previously reported high affinity for N_2O (Yoon et al. 2016).

Goals and research approach

The goals of this thesis are

(i) understand which mechanisms select for non-denitrifying N_2O-reducers (specialists) in open mixed-communities, i.e. what is their competitive advantage, and

(ii) elucidate what is the effect of excess or limitation of N_2O on the metabolism of the selected microorganisms.

To do so, the influence of the substrates availability and the growth rate on the selection of generalists or specialists N_2O reducers has been assessed.

Two continuously-fed stirred-tank membrane reactors (CSTMR) were run under either acetate or N_2O limiting conditions. Acetate was used as the carbon source to avoid the growth of fermentative organisms. Additionally, in order to get insight on the abovementioned finding in (Conthe, Wittorf, Kuenen, Kleerebezem, Van Loosdrecht, et al. 2018), a large SRT (7 days) was imposed. Ultrafiltration membranes were used to decouple the solids and the hydraulic retention time (SRT, HRT), allowing the growth of microorganisms with lower growth rates. The evolution of the microbial communities in the two reactors was monitored on multiple levels so that the abundance and diversity of microorganisms and its denitrifying and N_2O-reducing capacity could be characterized.

Inspiration

The modularity of the nitrogen cycle has been proved in multiple occasions (Costa et al. 2006; Roco et al. 2017), and several theoretical approaches have tried to explain why it is found in nature (D. Johnson et al. 2012; Pfeiffer et al. 2004). However, the reason behind it remains still unknown, hindering us from a deep understanding of the abundance and interactions of the species involved. This is the challenge I undertook in my thesis.

2. MATERIALS AND METHODS

2.1. Continuous-flow stirred-tank membrane reactor (CSTMR) operation (for enrichment of non-denitrifying N_2O-reducers)

Two 3L jacketed glass reactors with a working volume of 2L (Applikon, Delft, the Netherlands) were operated as continuous-flow stirred tank reactors under acetate- or N_2O-limiting conditions during 137 and 95 days respectively. The inoculum was obtained from an anaerobic digester in a wastewater treatment plant (Harnaschpolder, Delft, the Netherlands). The inflow was controlled by two peristaltic pumps feeding the carbon and nitrogen sources separately. The influent medium contained 45.3 mmol $NaCH_3COO{\cdot}3H_2O$, 13.3 mmol NH_4Cl, 7.4 mmol KH_2PO_4, 2.1 mmol $MgSO_4{\cdot}7H_2O$, 0.5 mmol NaOH, 2 mg yeast extract and 2.5 ml trace element solution (Vishniac et al. 1957) per liter. A hollow fiber membrane with 0.1 µm pore size was installed in order to control the solids retention time (SRT) and decouple it from the hydraulic retention time (HRT). An SRT of 7 days was controlled by a peristaltic pump extracting biomass-containing medium, while the HRT (3 days) was maintained by an effluent pump connected to the membrane and a sensor level.

The temperature of the reactor was maintained at 20 ± 0.1 °C using a cryostat bath (Lauda, Lauda-Königshofen, Germany). The pH was monitored with a pH electrode (AppliSens) and maintained at 7 ± 0.1 with 1M HCl and 1M NaOH solutions by an in-Control biocontroller (Applikon). The reactor was stirred at 750 rpm by two six-bladed flat turbines. The gas inflow was defined by two mass-flow controllers 5850S (Brooks,Philadelphia,USA) controlling the N_2O and N_2 gas flows. The k_La was determined to be 16-25 h^{-1} (see Section 7.1.). A DO probe was used to monitor whether anoxic conditions were maintained during the whole operational period.

The reactor was operated under non-sterile conditions. The biofilm generated on the membrane and on the reactor walls was cleaned every week. A scheme of the set-up is depicted in Figure 2, and a summary of the conditions can be found in Table 1.

R_2 operation started at day 52, when it was inoculated with biomass originating from R_1.

Table 1. Summary of the operating conditions of the two chemostat reactors. The parameters were calculated during the steady-state of each reactor: days 17-48 and 65-94 for R_1 and R_2 respectively.

Reactor	N_2O/CH_3COO^- ratio [mol·mol^{-1}]	Limitig nutrient	Days	HRT [d]	SRT [d]	Concentration in the reactor		
						CH_3COO^- [mM]	N_2O [off gas %]	Biomass [gVSS·L^{-1}]
R_1	10.3	Acetate	137	2.9 ± 0.4	7.0 ± 1.1	< 0,1	1.3 ± 0.3	0.82 ± 0.14
R_2	2.7	N_2O	95	2.9 ± 0.4	6.9 ± 0.8	25.54 ± 1.91	0.065 ± 0.003	0.84 ± 0.09

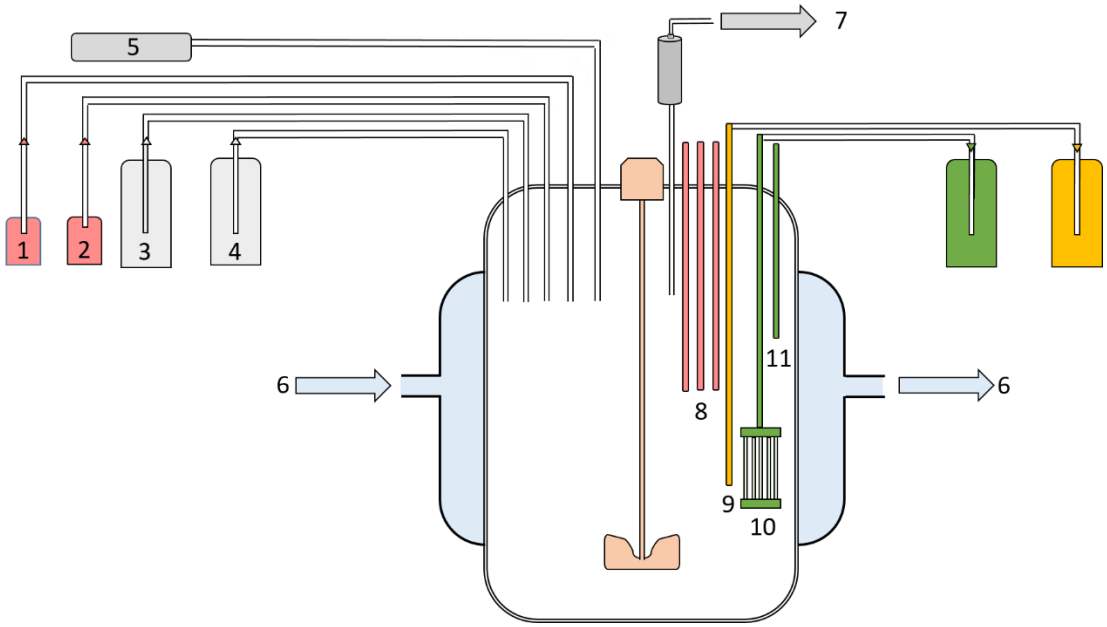

Figure 2. Schematic representation of the set-up used during the CSTMR experiments. The membrane allows to decouple SRT and HRT, enhancing the presence of microorganisms with low growth rates. 1. Acid pump. 2. Base pump. 3. N-source. 4. C-source. 5. In-gas. 6. Cooling water in the jacket. 7. Off-gas. 8. DO, T, pH probes. 9. SRT/sampling port. 10. HRT port/membrane. 11. Level sensor.

2.2. Batch test: denitrification activity of the N_2O-reducers

The denitrification activity of the chemostat cultures was followed performing batch tests. 350 mL of the reactor content was centrifuged at 4200 rpm for 20 min at 20ºC. The pellets were resuspended in medium to a final mass of 350 g, achieving a biomass concentration of 0.9 ± 0.2 $g \cdot L^{-1}$. The medium contained 7.4 mmol KH_2PO_4, 2.1 mmol $MgSO_4 \cdot 7H2O$, 0.5 mmol NaOH, 2 mg yeast extract and 2.5 ml trace element solution (Vishniac et al. 1957) per liter. 100 mL flasks were filled with 50 mL of the solution. Anoxic conditions were achieved by flushing with pure N_2 for 20 min at 500 $mL \cdot min^{-1}$. The culture was maintained overnight at 20 ºC and shaken at 150 rpm. The batch assays started after injecting NH_4Cl (and $NaCH_3COO \cdot 3H_2O$) to reach 30 mg $NH_4^+ \cdot L^{-1}$ and 1 mmol $CH_3COO^- \cdot L^{-1}$. During this period the N_2O-independent acetate consumption of the culture was assessed. After 3h, the flasks were spiked with $NaNO_2$ to reach a concentration of 20 mg $N \cdot L^{-1}$. A negative control to account for other forms of N_2O consumption such as adsorption or chemical reduction was carried out using dead (autoclaved) biomass. All assays were performed in duplicate. A schematic representation of the three different cases is depicted in Figure 3

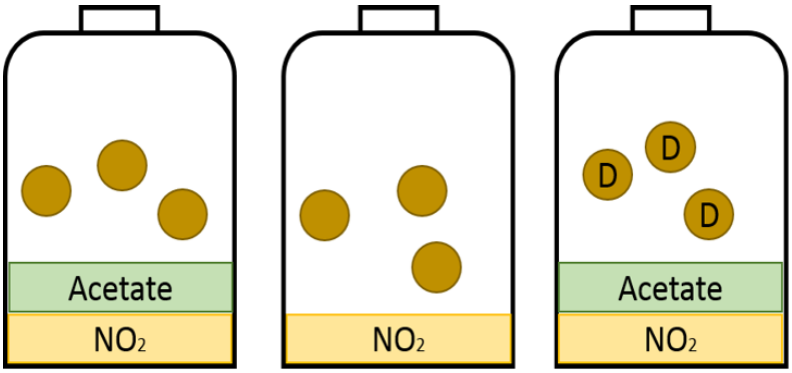

*Figure 3. Schematic representation of the three types of bottles used during the batch test. **Left**: acetate, nitrite and alive biomass. **Center**: control A. Acetate was not present. The goal was to calculate the NO_2 consumption with endogenous COD. **Right:** control B. Goal: calculate the NO_2 disappearance related to physicochemical (adsorption, absorption) or biological processes not related to denitrification. In all cases, ammonia was added to the medium to prevent N2 fixation.*

The samples were centrifuged at 4ºC, 13000 rpm during 3 min and stored at -20 ºC after discarding the pellet. The N_2O and acetate concentrations were measured as explained below in less than 6 days after collection.

2.3. Analytical procedures

The biomass concentration was estimated by measuring the volatile suspended solids (VSS) and assuming a biomass composition of $CH_{1,8}O_{0,5}N_{0,2}$ unless specifically stated (Roels 1980). 100 mL was sampled from the reactor and centrifuged at 4200 rpm for 20 min. After discarding the supernatant, the pellet was dried at 105 ºC and ashed at 550 ºC for at least 24 and 2 hours, respectively.

Acetate was measured using a Waters 717Plus high-pressure liquid chromatograph (HPLC) with an infrared detector and an HP Innowax column (Waters, MA, USA). Ammonium, NO_3^- and NO_2^- concentrations were determined spectrophotometrically using a GalleryTM Plus Discrete Analyser (Thermo Fisher Scientific, Massachusetts, USA).

The composition of the reactor off-gas was analysed using a Rosemount off-gas analyser (Emerson, Missouri, USA) or with a CP-3800 gas chromatograph (Varian, CA, USA).

Biomass for polyhydroxyalkanoate (PHA) determination was collected and centrifuged at 4200 rpm for 20 min before discarding the supernatant and drying at 60ºC for 3 days. The PHA content was determined using a gas chromatograph (Agilent 6890N, USA) equipped with a flame ionization detector (FID) and a HP-INNOWax column. A solution of 14% poly-(3-hydroxybutyric acid-co-3-hydroxyvaleric acid) (Sigma-Aldrich, CAS 80181-31-3) was used as a standard to calculate the PHA content and benzoic acid as the internal standard. A detailed description of the procedure can be found in (K. Johnson et al. 2009).

PHA imaging was carried out with light microscopy (Axioplan 2, Zeiss, Sliedrecht, the Netherlands). Images were acquired using a Zeiss MRM camera and compiled with the Zeiss microscopy image acquisition software (AxioVision version 4.7, Zeiss).

Elemental and electron balances were set up to determine the conversion taking place in the chemostat and during the PHA fermentation experiment. The N_2O, and CO_2 off-gas concentrations were computed from the off-gas partial pressure and the gas supply rate. Both dissolved N_2O and CO_2 were taken into account in the balances, as well as the PHA fraction in the biomass.

2.4. DNA extraction and quantitative PCR of *nirK, nirS, nosZ*, and 16S rRNA genes

DNA was extracted from pellets obtained from 2 mL of the reactor content using the PowerLyzer PowerSoil DNA Isolation Kit (MolBio Laboratories) according to manufacturer instructions. DNA concentration was quantified using the Qubit Fluorimeter (Life Technologies Corporation).

The genes *nirS, nirK, nosZI, nosZII* and 16s rRNA were quantified via quantitative real-time PCR (qPCR) to determine the denitrification and N_2O-reducing genetic potential of the cultures. Each well contained 5 ng template DNA, 10 µL iQ SYBR Green Supermix (BioRad), 0.1% BSA, and primer concentrations of 0.25 $\mu mol \cdot L^{-1}$ for *nirK*, 0.5 $\mu mol \cdot L^{-1}$ for *nirS* and 16S rRNA, and 0.8 $\mu mol \cdot L^{-1}$ for both *nosZI* and *nosZII*. Primer sequences as well as qPCR recipes can be found in Table S 2.

Standard curves were obtained analysing serial dilutions of each of the genes. The genes were obtained amplifying (PCR) them from the genome of three different samples of R_1. The protocol used for the PCR is the same as for the qPCR. Electrophoresis gels were run to check the purity of the PCR products obtained. Images of each of the gels can be found in Section 7.7. , Figure S 8.

2.5. Amplicon sequencing of 16s rRNA genes

The microbial diversity of the chemostat cultures was characterized by amplicon sequencing of the 16s rRNA genes. The primers used can be found in Table S 2. Samples were sent to Novogene Ltd. (Hongkong, China) for amplicon sequencing of the V3-4 region of the 16S-rRNA gene (position 341-806) on an Illumina paired-end platform. After sequencing, the raw reads were quality filtered, chimeric sequences were removed and OTUs were generated on the base of ≥ 97% identity. Subsequently, microbial community analysis was performed by Novogene using Mothur & Qiime software (V1.7.0). For phylogenetic determination the most recent SSURef database from SILVA (http://www.arb-silva.de/) was used.

Samples are currently being analysed at the moment of the submission of the thesis.

3. RESULTS AND DISCUSSION

3.1. CSTMR operation: conversion rates and biomass yields

Acetate and nitrous oxide limitations select for two different microbial communities

Two 2-L continuous-flow stirred-tank membrane reactors (CSTMR) were run under acetate (R_1) and N_2O (R_2) limiting conditions during 137 and 93 days, respectively. A custom-made microfiltration membrane module (pore size of 0.1 µm) allowed uncoupling the control of HRT (2.9 ± 0.4; 2.9 ± 0.4 d) and SRT (7.0 ± 1.1; 6.9 ± 0.8 d) for R_1 and R_2, respectively. Acetate was never detected in the acetate-limited reactor, and concentrations of N_2O <700 ppm were found in the off-gas of the N_2O-limited one. N_2O limitation was confirmed by decreasing the N_2O load and measuring the consequent decrease in biomass concentration and increase in effluent acetate (days 15-20, Figure S 7). Images of the two reactors are shown in Figure 4. Already the difference in the colour of the two reactors suggests that the composition of the microbial communities was different.

Figure 4. Image of broth of the two reactors during the steady-state. ***Right.*** *R_1, acetate-limited.* ***Left****. R_2, N_2O-limited. The pressure created in the two reactors selected for different microbial communities, as suggested by the difference in colour (white and dark grey, respectively).*

The conversion rates during the steady state are presented in Table 2. Over 75% recovery for both carbon and electrons was obtained in R_2. This calculation cannot be done for R_1, since the off-gas concentrations of CO_2 and N_2O could not be accurately obtained. Interestingly, polyhydroxyalkanoates (PHA) were consistently found in the two reactors at significant percentages, as supported by microscopy (Section 7.4. Figure S 3) and PHA extraction. Thus they have been included in the carbon and electron balances. As methane production cannot be excluded a-priori under the conditions of R_2, methane concentration in the off-gas was measured on days 139-145 and confirmed to be negligible (< 1% of incoming C). To discard the presence of sulphate reducers, the concentration of sulphide (S^{-2}) was measured as well, and proved to be negligible as well.

Table 2. Average conversion rates in the chemostats during the steady-states. Negative numbers indicate consumption; positives, production. Carbon (C) and electron (e-) balances indicate recovery.

Reactor	Limiting nutrient	Compound conversion rates [mmol·h^{-1}]						C-bal [%]	e$^-$-bal [%]
		CH_3COO^-	N_2O*	N_2	NH_4^+	$CH_{1.8}O_{0.5}N_{0.2}$	CO_2		
R_1	Acetate	-32.24 ± 0.84	-193.6 ± 24.4	-	-4.20 ± 0.98	9.03 ± 1.05	-	-	-
R_2	N_2O	-26.99 ± 1.44	-81.7 ± 0.4	81.51	-5.72 ± 1.06	8.58 ± 0.51	33.20 ± 2.16	79	103

**Due to the high uncertainty associated to the obtained values for the off-gas N_2O concentration, this value is only used to qualitatively confirm that N_2O was consumed.*

The N_2O:acetate ratio consumed by R_2 is 3.1 mol·mol^{-1}, in accordance with the results of (Conthe, Wittorf, Kuenen, Kleerebezem, Van Loosdrecht, et al. 2018). Moreover, approximately 50% of the acetate consumed was released in form of CO_2.

Coping with excess N_2O seems to be an extra cellular burden

In order to further explore the difference in the yields, the maintenance coefficients of the two cultures were calculated combining the data hereby presented with the one in (Conthe, Wittorf, Kuenen, Kleerebezem, Van Loosdrecht, et al. 2018). Maintenance is defined as *the energy consumed for functions other than the production of new cell material* (Pirt 1965). Therefore, if the abovementioned toxicity of N2O is playing a role in the microbial community, extra energy and resources must be employed to fix its effects, which represents an additional metabolic burden for the cells and translate into a higher maintenance coefficient. The results presented in Table 3 support this hypothesis, as maintenance in R1 was 30% higher than in R2. More information can be found in Section 7.3.

Table 3 shows the biomass yields on acetate and nitrous oxide of the two reactors, as well as the ones found by (Conthe, Wittorf, Kuenen, Kleerebezem, Van Loosdrecht, et al. 2018). In the present work, the biomass yield on acetate differs considerably between the two conditions. More precisely, it is lower when N_2O is provided in excess: 0.14 and 0.17 CmolX·CmolS^{-1} under acetate- and N_2O-limited conditions, respectively. The same trend was observed for nitrous oxide. The biomass yield on this compound is lower when N_2O is present in excess (acetate-limiting conditions) than under N_2O-limiting conditions. This phenomenon was also observed in (Conthe, Wittorf, Kuenen, Kleerebezem, Van Loosdrecht, et al. 2018), where the difference was attributed to the toxicity of N_2O. This compound has been characterized as an inhibitor of the cobalamin-dependent methionine synthase (MS), important in DNA synthesis (Hansen 1986; Taylor 1982; Weimann 2003). Specifically, N_2O oxidizes the cobalt ion of cobalamin, the cofactor of MS. This enzyme catalyses the production of methionine and tetrahydrofolate (THF), essential for methylation and purine and thymidine synthesis, respectively (Nagele et al. 2008). A schematic representation of this inhibition is shown in Figure 5

Table 3. Biomass yields and maintenance coefficients obtained during the steady-state of the two cultures in this work and in (Conthe, Wittorf, Kuenen, Kleerebezem, Van Loosdrecht, et al. 2018).

Source	Limiting nutrient	SRT [d]	Y_{XAc} [CmolX·CmolS^{-1}]	Y_{XN2O} [CmolX·molN$_2$O^{-1}]	Y_{XNH4+} [molN·CmolX^{-1}]	Maintenance coefficient [CmolS·CmolX^{-1}·h^{-1}]
This work		7.0 ± 1.1	0.13 ± 0.01	0.05**	0.38 ± 0.08	
Conthe *et al.,* 2018*	Acetate	1.49 ± 0.05	0.25 ± 0.02	0.16 ± 0.01	0.28 ± 0.02	0.023
Conthe *et al.,* 2018*		0.47 ± 0.002	0.27 ± 0.01	0.17 ± 0.01	0.28 ± 0.01	
This work		6.9 ± 0.8	0.17 ± 0.02	0.11 ± 0.01	0.47 ± 0.07	
Conthe *et al.,* 2018*	N_2O	1.49 ± 0.05	0.32 ± 0.04	0.22 ± 0.04	0.26 ± 0.01	0.018
Conthe et al., 2018*		0.47 ± 0.002	0.33 ± 0.03	0.26 ± 0.02	0.28 ± 0.02	

* (Conthe, Wittorf, Kuenen, Kleerebezem, Van Loosdrecht, et al. 2018)

***Due to the high uncertainty associated to the obtained values for the off-gas N_2O concentration, this value is only used to qualitatively confirm that the biomass yield on N_2O is higher under N_2O-limiting conditions than under acetate limitation.*

Surprisingly, the biomass yield on ammonia is considerably higher than expected (0.2 molN·CmolX^{-1} assuming the standard biomass composition $C_1H_{1.8}O_{0.5}N_{0.2}$). Nevertheless, similar yields were reported for *Pseudomonas stutzeri* in (Conthe, Wittorf, Kuenen, Kleerebezem, Van Loosdrecht, et al. 2018), a well-known denitrifying species. The underlying reasons for this observation remain unclear, and warrant further research. Characterization of the biomass composition is highly recommended.

Interestingly, there is an inverse relationship between SRT and biomass yield on N_2O and acetate for each of the conditions. This correlation has been found in several other ecological contexts (Lipson et al. 2009; Sorokin et al. 2003), and it is based on the different distribution of resources (e.g. carbon, energy). At high growth rates, most of the energy is invested in growing. On the other hand, low growth rates lead to the use of a bigger portion of the energy for maintenance purposes (Pirt 1965), resulting in a lower biomass yield.

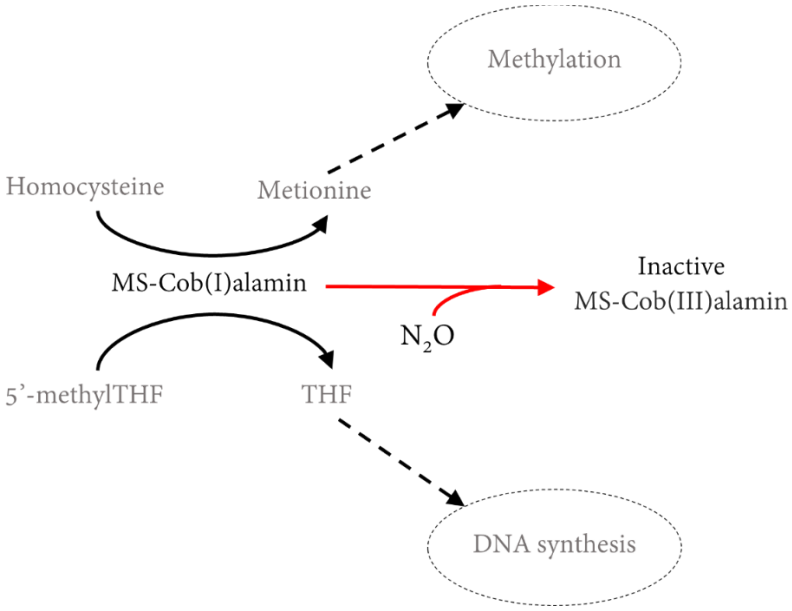

Figure 5. Effect of N_2O on the cellular metabolism. Methionine synthase (MS) catalyses the conversion of homocysteine and 5'-methyltetrahydrofolate into methionine and tetrahydrofolate. These metabolites are essential for the methylation and DNA synthesis processes. Cobalamin, the cofactor of MS, contains a cobalt ion in its reduced form (Co^{1+}),which is required for the catalytic activity of MS. N_2O oxidizes Co^{1+} to Co^{3+}, inactivating MS and thus hindering the synthesis of biomass. Adapted from Nagele et al., (2008).

In order to further explore the difference in the yields, the maintenance coefficients of the two cultures were calculated combining the data hereby presented with the one in (Conthe, Wittorf, Kuenen, Kleerebezem, Van Loosdrecht, et al. 2018). Maintenance is defined as *the energy consumed for functions other than the production of new cell material* (Pirt 1965). Therefore, if the abovementioned toxicity of N_2O is playing a role in the microbial community, extra energy and resources must be employed to fix its effects, which represents an additional metabolic burden for the cells and translate into a higher maintenance coefficient. The results presented in Table 3 support this hypothesis, as maintenance in R_1 was 30% higher than in R_2. More information can be found in Section 7.3.

This hypothesis could be experimentally tested by measuring the relative abundance of intact methionine synthase at different concentrations of N_2O. This could be achieved using mass spectrometry (Han et al. 2009). Direct addition of cobalamin in the medium would not enhance the cellular performance, since most likely it would be oxidized by the excess of N_2O.

In conclusion, growth under excess N_2O results in lower biomass yields on acetate and N_2O in comparison to N_2O limitation. Moreover, the energy used for non-growth processes (i.e. maintenance coefficient) is higher, strongly supporting the hypothesis that N_2O interferes negatively with the cellular metabolism.

3.2. Denitrification activity and functional genes abundance of the communities

Selecting for specialists N_2O reducers implies washing out the microorganisms able to produce N_2O while maintaining the ones able to (only) consume it. From a genetic point of view, this implies obtaining a culture that *(i)* possesses *nosZI* or *nosZII*, the enzymes able to reduce N_2O to N_2, and *(ii)* lacks *nar, nir* and *nor,* the genes encoding the catalytic enzymes in the denitrification pathway (Kuypers et al. 2018). In the present work, the focus was put on *nirS* and *nirK*, responsible for the reduction of NO_2^- to NO, the reaction commonly used as a proxy for denitrification (Ji et al. 2015; Zumft 1997). Since N_2O is consumed in the reactor, the first goal was achieved. In order to get insight on the second one, the relative abundance of the abovementioned genes was quantified, and the specific denitrification activity of the cultures was assessed via batch test on a weekly basis. The trends found in the two reactors are shown in Figure 6.

Specific denitrification activity was not washed out

The specific denitrification activity of the two microbial communities stabilized at a similar value of 1.1 mol NO_2-N·CmolX^{-1}·h^{-1} Figure 6, Panels A, B). At the start of the culture and after each perturbation (depicted as a grey area), the activity decreased. This was observed twice in R_1 (data not shown) and three times in R_2. However, the denitrification activity was never completely lost, and was maintained stable during three SRT in both cases.

Total nir/nosZ genes ratio shows that the affinity for N_2O does not enrich for N_2O-reducing capacity under the imposed conditions

The relative abundance of *nir* (*nirS* + *nirK*) was the same in the two reactors as well, and similar to the one found by (Conthe, Wittorf, Kuenen, Kleerebezem, Van Loosdrecht, et al. 2018). This shows that the

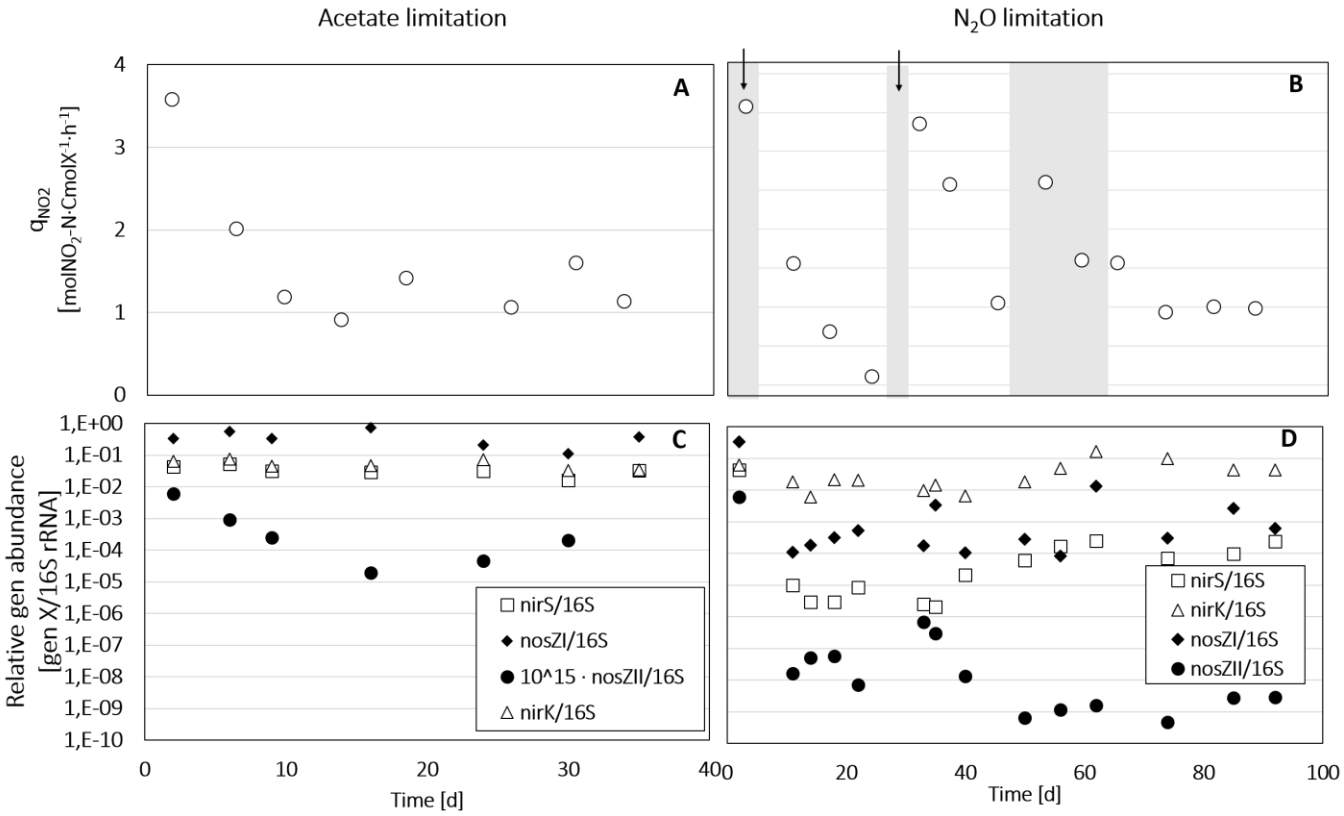

Figure 6. ***Top.*** *Specific denitrification activity of the microbial communities under acetate (R_1, A) and N_2O limitation (R_2, B).* ***Bottom****. Relative abundance of functional genes* nirS, nirK, nosZI and nosZII *over* 16S rRNA *under acetate (R_1, C) and N_2O (R_2,D) limitation. The specific denitrification activity stabilized at similar values in the two reactors in two different periods of time (one of them not shown in R_1). The relative abundance of* nirK *was similar under both conditions, while the ones of* nirS *and* nosZI *decreased three orders of magnitude under N_2O limitation compared to acetate limitation. During the same period, the presence of* nosZII *was 12-14 orders of magnitude higher when N_2O was limiting than when acetate was. The first black arrow (↑) in panel B points at the inoculation time of R_2, while the second one shows when R_2 was inoculated with some (15 wt% of R_2) biomass from R_1 to compensate for the decrease in biomass due to the low N_2O flux used during the previous days. More information can be found in Section 7.6. and Figure S 7. Grey areas highlight the time periods when technical problems occurred.*

denitrifying N_2O-reducers (generalists) were not washed out from the reactor, regardless of the limiting substrate. Moreover, it validates the use of the presence of *nir* as a proxy for denitrifying capacity, in contrast to the observation of (Veraart et al. 2017) that *nir* abundance does not correlate with denitrification activity.

The relative abundance of *nos* (*nosZI* + *nosZII*) was higher when acetate was limiting than when N_2O was, in line with the higher N_2O conversion rate found in R_1 (Table 2). Yet, the biomass yield on N_2O was lower. Moreover, and contrary to our expectations, the ratio *nosZ/nir* was higher than unity and than the one obtained under N_2O limitation. Since N_2O was not the limiting substrate, all these findings suggest that the high *nosZ* relative abundance found in R_1 is linked to detoxification purposes and not to energy conservation. Based on this, we hypothesize that the ability to cope with N_2O cytotoxicity could play an important role as selecting factor, together with affinity for N_2O and maximum growth rate.

Conversely, the ratio *nosZ/nir* was constantly lower than unity under N_2O-limiting conditions. Thus, under the imposed conditions (i.e. SRT of 7 d) the affinity for N_2O (defined as μ_{max}/K_s) did not result in the enrichment of a community with high N_2O reducing capacity. This confirms the results of (Conthe, Wittorf, Kuenen, Kleerebezem, Van Loosdrecht, et al. 2018), who observed that generalists N_2O-reducers were favoured over specialists when N_2O was the sole electron acceptor, regardless of the limiting substrate. Interestingly, similar ratios were found by (Conthe, Wittorf, Kuenen, Kleerebezem,

Hallin, et al. 2018) at lower SRTs (1.5 d). In addition, a high (10^5) *nosZI/nosZII* was obtained, contradicting the results of Yoon *et al*. (2016), who stated that organisms harbouring *nos*Z clade II have a higher affinity for N_2O than those with *nosZ* clade I.

Affinity for N_2O selects for organisms with clade II nosZ *under the imposed conditions*

The affinity (defined as μ_{max}/K_s) for N_2O is a selective parameter for organisms harbouring *nosZII* under the tested conditions. The abundance of this gene raised by 12-14 orders of magnitude when the microbial community in R_1 was enriched under N_2O limitation in R_2. In parallel, *nirS* and *nosZI* abundances decreased by three order of magnitude under these conditions. Interestingly, in natural ecosystems, the percentage of organisms possessing *nosZI* that also harbour *nirS* is significantly higher than the ones with *nirK*, and thus represent the biggest fraction of the denitrifying N_2O-reducers (generalists) (Graf et al. 2014). Conversely, the presence of *nirK* was similar regardless of the limiting substrate, and this was the most abundant functional (quantified) gene in the community enriched under N_2O limitation. However, the multiple DNA fragments found in its amplification product (Figure S 8) hinder the reliability of these results. The design of alternative primers is highly recommended.

Last, we cannot exclude that the use of acetate as carbon source and electron donor impacted the selection of the microbial community. In this perspective, studies targeting different and more complex substrates are required. An additional limitation of the method is the use of 16S rRNA to calculate the relative abundance of the functional genes. The number of copies of this gene is highly variable among species, and thus can constitute an additional source of bias (Louca et al. 2018). The use of metagenomics would give a more accurate result on the abundance of the genes.

3.3. Accumulation of storage compounds

Polyhydroxyalkanoates (PHA) are carbon, energy and reducing-power storage materials accumulated by bacteria. PHA are synthesized under unbalanced growth conditions, usually when an essential growth component such as N or P is missing in the presence of excess carbon (Salehizadeh et al. 2004). PHA comprise different compounds such as polyhydroxybutyrate (PHB) or polyhydroxyvalerate (PHV) (A Steinbiichel 1992)(Alexander Steinbiichel 1991). Accumulation capacity is widespread among bacteria, and PHA storage has been widely reported for denitrifying communities (Beun et al. 2000; Liu et al. 2015; Seviour et al. 2000). Up to 90 wt% PHA accumulation (g PHA· g biomass^{-1}) has been achieved in open mixed cultures under feast/famine conditions and SBR operation (K. Johnson et al. 2009). In these systems, fast storage capacity is a key factor in the competition for substrates between microorganisms, for only the ones that accumulate PHA survive the famine phase (Reis et al. 2003). Nevertheless, several studies also reported the accumulation of PHA in continuously-fed systems (Cavaillé et al. 2016; Wen et al. 2010). Conversely, the competition under these conditions is driven by the affinity of the microorganisms for the limiting substrate. An excellent overview can be found in (Korkakaki et al. 2017).

In the present work, consistent and stable PHA accumulation was observed both under N_2O- and acetate-limiting conditions. PHA accounted for 4.9 ± 0.7 and 7.8 ± 0.4 per cent of the total biomass dry weight in R_1 and R_2, respectively. The PHA in both reactors displayed similar compositions; PHB and PHV

represented 78 ± 6 and 22 ± 5 per cent of the total PHA content. Different explanations[1] for the accumulation in the two reactors are proposed.

Electron acceptor limitation triggers the synthesis of polyhydroxyalkanoates (PHA)

Several studies have reported PHA accumulation in continuously-fed systems with acetate excess and a limiting growth essential component (Egli 1991; Frank 1999). However, in agreement with (Senior et al. 1972, 1973; Ward et al. 1977) it is reasonable to assume that in the present work PHA accumulates in R_2 due to the electron acceptor (N_2O) limitation. Senior *et al.,* (1972) showed that in an aerobic, continuous system with carbon excess, oxygen limitation resulted in the synthesis of PHA. This synthesis responded to the demand of an electron sink into which the excess of reducing power could be channelled. In analogy, we propose that in this work PHA synthesis might be used to control the cellular NADH, NADPH, ATP and CoA pools. The residual concentrations of $NH_4^+$and PO_4^- in the effluent further support this hypothesis.

A simplified scheme of the cell metabolism if depicted in Figure 7. As previously mentioned, acetate is the only electron donor in the system. Thus, the first step in the cell catabolism is its import, which can be either active (involving the consumption of 1 mol ATP per mol acetate) or passive or facilitated (without ATP consumption)(Casal et al. 1996; Filipe et al. 2001). This acetate is then converted to acetyl-CoA at the expense 1 mol ATP per mol acetyl-CoA (Beun et al. 2002; Stouthamer 1973). Acetyl-CoA enters the tricarboxylic acid (TCA) cycle, yielding reducing-power (NADH), CO_2 and CoA (Lehninger et al. 1993). This reducing power can then be invested in the electron transport chain (ETC), which results in the generation of ATP via reduction of N_2O to N_2 (Pauleta et al. 2019). Finally, biomass can be produced using this ATP and other growth essential components. Overall, acetate and nitrous oxide provide the energy required for cell growth.

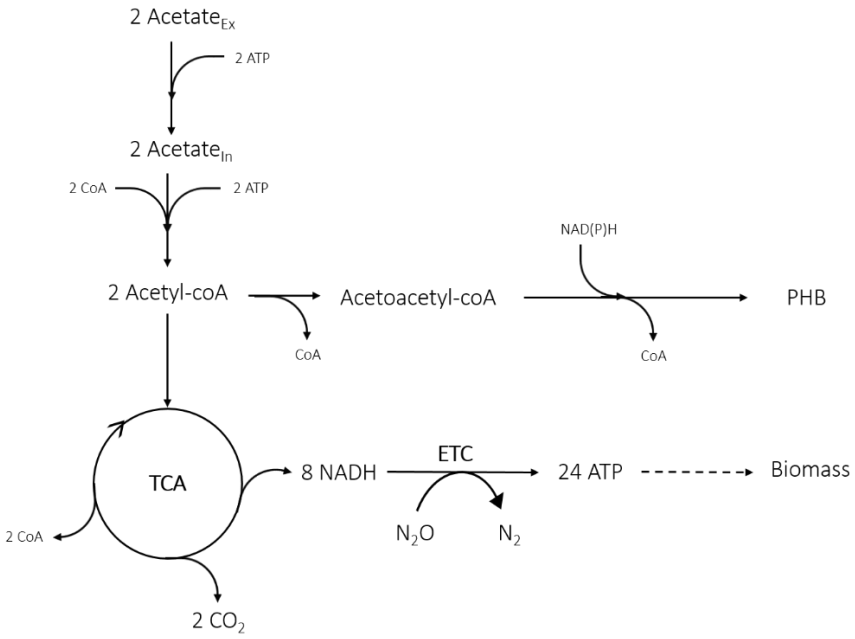

Figure 7. Schematic overview of the metabolism of the microbial communities obtained in R_1 and R_2. After its import, acetate is converted into acetyl-CoA, which can then be used to generate energy in the TCA and the ETC, to generate PHB or to produce biomass. The availability of the cofactors ATP, NAD(P)H and CoA will determine the flux through each of these pathways. Adapted from Third et al.,(2003).

[1] Since PHB accounted for ca. 80% of the PHA, the analysis of the PHA metabolism performed in this section takes only PHB into account.

All the above mentioned processes are dependent on the intracellular pools of certain molecules. ATP and NADH are well-known indicators of the cellular metabolic state. While the ATP/AMP ratio represents the cellular energy (Hardie 2015), NAD^+/NADH reflects the redox status (Houtkooper et al. 2010). Recently, it was discovered that acetyl-CoA (CoA) plays a similar role (Shi et al. 2015). In the cells, metabolic fluxes are balanced so that the concentrations of these components are in equilibrium. Consequently, the absence of electron acceptor (N_2O) in R_2 will alter the cellular metabolism, leading to a redistribution of the resources that will balance the concentration of those key metabolites. Similar behaviours were found in (Locasale et al. 2011), where the activity of lactate hydrogenase responded to the NAD^+/NADH balance, and in (Larsson et al. 2000), where the glycolytic flux varied with the ATP levels.

The lack of electron acceptor will directly impact the flux through the ETC, restricting the ATP synthesis and resulting in the accumulation of NADH. Consequently, the TCA cycle flux will also be diminished, causing the accumulation of acetyl-CoA and the subsequent decrease in the CoA levels. This leaves the cell with high levels of reducing-power and low CoA. The production of PHA requires reducing-power and results in the release of CoA (Third et al. 2003) . Moreover, high acetyl-CoA/CoA ratios were recently shown to be essential for the thermodynamic feasibility of the PHB production (Velasco et al. 2019). Therefore, PHA synthesis could re-establish the CoA and NADH pools. In conclusion, it is reasonable to assume the observed production of PHB to be a consequence of the cellular need to maintain the ratios of the above mentioned key metabolites.

Two aspects are worth highlighting and warrant further analysis. First, the cofactor produced in the TCA, NADH, is not the one typically consumed in the PHB synthesis (NADPH) (Miyahara et al. 2018). However, an NADH-dependent pathway for the synthesis of PHB has been shown to exist (Amos et al. 1993; A Steinbiichel 1992), and its use was associated to the PHB production under electron-acceptor limitation (Ling et al. 2018). Enzymatic assays will be carried out to identify the specific reducing factor for PHB production in the selected organisms. The presence of transhydrogenases, which allow the conversion of NADH into NADPH, could also allow to overcome this limitation and link the two processes (Dawes 1988).

Second, acetate uptake by the cell can be passive (in protonated form) or active (with the consumption of 1 ATP) (Konings 1977). If transport were active, incoming flux could be controlled and balanced with the availability of electron acceptor. This would limit acetyl-CoA accumulation, and most likely result in negligible PHA accumulation. Conversely, if transport were passive, acetate would be driven by the difference between the extra- and intracellular concentrations, and thus the PHB production would be required.

In order to further understand this phenomenon, the actual acetate concentration in the reactor was raised by increasing the ratio acetate/N_2O, resulting in a higher acetate concentration in the liquid. This was achieved by either increasing the acetate concentration in the medium (days 112 – 117, Figure 8) or decreasing the N_2O concentration in the influent gas (days 68 – 77). As shown in Figure 8, in both cases this resulted in a higher PHA content, strongly supporting the fact that acetate uptake is passive and thus proportional to the extracellular concentration.

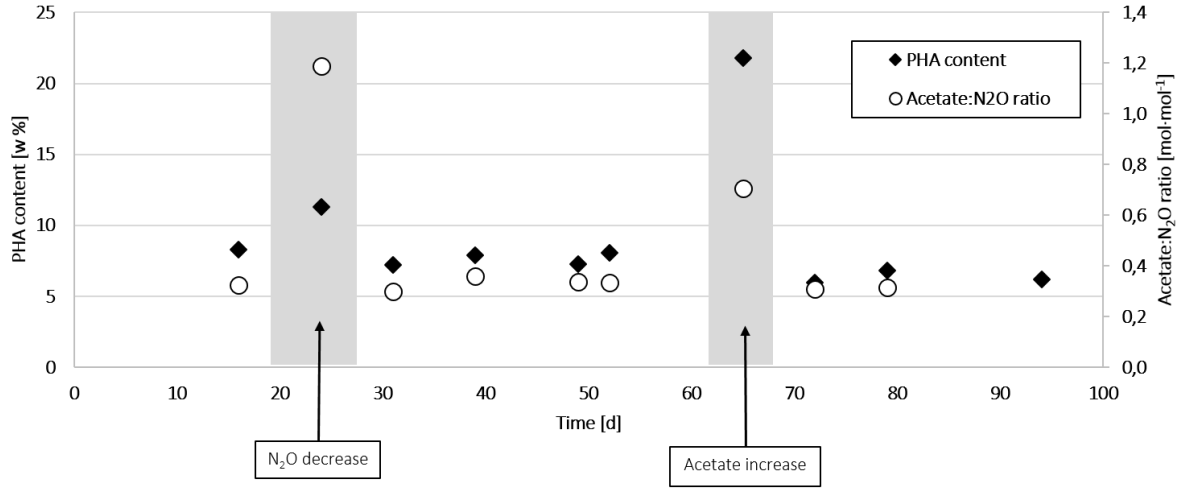

Figure 8. Cellular PHA content [w%] and molar acetate:N_2O ratio in the feed of R_2 (N_2O-limited). PHA content is stable as long as the C:N_2O ratio is constant, yet it is sensible to its changes. An increase in the ratio boosts PHA accumulation, regardless of which of the flowrates is manipulated.

Studies on the impact of pH would help to gain a better insight. A lower pH would increase the concentration of the protonated form of acetate, which should lead to a higher PHA content. The opposite is expected if the experiment was carried out at a higher pH.

N_2O toxicity leads to PHA synthesis

Polyhydroxyalkanoates granules were also observed in R_1, where acetate was always limiting. PHA accumulation under acetate limitation was also observed by Cavaille, 2016, where accumulation was shown to be the result of a dual C-P limitation. Specifically, the biomass concentration was limited by the amount of P provided, and as a result the excess of acetate was stored as PHA. In the present work, NH_4^+ and PO_4^- were present in the effluent of both reactors. Other elements were not measured, and thus dual limitation cannot be excluded. At the same time, it is tempting to speculate that PHA accumulation in R_1 is the result of the partial toxicity of N_2O discussed before (Section 3.1.).

In analogy to P or N limitation, partial toxicity could limit the growth. N_2O inactivates methionine synthase (MS) (Hansen 1986; Taylor 1982; Weimann 2003), which is involved in the synthesis of DNA (Nagele et al. 2008). Therefore, MS scarcity hinders biomass production. Compared to the N_2O-limiting conditions, N_2O excess has resulted in lower biomass yield on acetate and higher maintenance costs (Pirt 1965), supporting this hypothesis. The increase in the maintenance costs might be associated to the activation/synthesis of (more) MS. A lower availability of MS would result in a diminished carbon flux directed to biomass synthesis. This would, in analogy to R_2, result in the accumulation of acetyl-CoA and the production of PHA.

This hypothesis warrants further research. Studying the effect of a step-wise increase or decrease in the N_2O gas flow on the PHA content is highly recommendable.

PHA is fermented under anaerobic conditions

Stored PHA can serve for different purposes such an energy production or biomass synthesis (Brigham et al. 2011). In the current study, the use of PHA by the R_1 enrichment was studied under anaerobic conditions. Incubation of PHA rich biomass under anaerobic conditions and in absence of any carbon and energy sources consistently resulted in acetate release (Figure S 4, Panel B). This phenomenon has been reported in literature and associated to PHA fermentation into volatile fatty acids (VFA) (Huda et al. 2016). Huda *et al.* (2016), described the process with microorganisms containing a 1:1 ($mol \cdot mol^{-1}$) mixture of PHB/PHV (or its monomers hydroxybutyrate (3HB) and hydroxyvalerate (HV)), and claimed that its fermentation followed equation 1:

$$2x\ 3HB + 2y\ HV \rightarrow (2x+y)\ acetate + y\ propionate + x\ butyrate + y\ valerate \qquad (1)$$

and yielded 0.5 mol ATP · mol PHA^{-1}. In order to further characterize the fermentation of PHA in the present work, R_1 was operated in batch mode under anaerobic conditions during 35h without any additional feed. Results are shown in Table 4. In accordance to Huda *et al*. (2016), acetate, propionate and butyrate were the main fermentation products, accounting for 101% of the PHA carbon loss. Intriguingly, 5-hydroxymethylfurfural (HMF) was also detected after 27 h, yet its implication in the PHA metabolism remains unknown. HMF is a C_6 compound typically formed during the dehydration of a broad variety sugars ranging from monosaccharides like fructose (Chen et al. 2014) to polysaccharides like cellulose (Zhao et al. 2011). Its reduction state (4) is lower than that of PHA (4.5), thus its production from PHA could yield energy to the cell. However, to our knowledge this pathway has not been described yet. Further investigation is needed to properly identify and quantify it. Both NMR and HPLC assays are suitable and thus recommended to do so.

Table 4. Total amount of PHA and VFAs in the reactor before and after the PHA fermentation experiment. All (101%) the carbon present in the fermented PHA was recovered in the form of VFAs.

Compound	Amount [Cmol]	
	t = 0 h	t= 35 h
PHA	4.39	2.18
Acetate	0.08	1.78
Butyrate	0.28	0.63
Propionate	0.13	0.31
Cmol PHA in VFA (%)	-	101

In conclusion, both cultures were capable of storing PHA in continuously-fed regime. Two different mechanisms are proposed to explain the reasons leading to its synthesis. In the first case, the lack of electron acceptor resulted in the accumulation of NADH and acetyl-CoA. The PHB synthesis acted as an electron sink and as a source of CoA, restabilising the levels of NADH and CoA. In the second scenario,

the partial toxicity of N_2O hindered the production of biomass, and the excess of ATP lead to high levels of NADH and acetyl-CoA. Again, PHB synthesis was utilized to re-establish the ordinary levels of these two cofactors. Additionally, the PHA fermentation capacity of the microbial communities was also proved and supported by literature. Under anaerobic conditions, PHA is fermented into acetate, butyrate and propionate, yielding energy in the form of ATP.

4. CONCLUSIONS

In the present work, the mechanisms selecting for specialist N_2O-reducers in natural environments and the effect of excess or limitation of N_2O on the cellular metabolism were investigated. To do so, two continuously-fed stirred-tank membrane reactors (CSTMR) were run at long SRTs (7 d) under either acetate or N_2O limiting conditions. The specific denitrification capacity of the microbial community and the relative abundance of genes encoding for NO_2 (*nir*) and N_2O (*nosZ*) reductases were monitored. Based on the obtained results, several conclusions can be drawn.

A long SRT (7 days) was imposed to allow for slower growing organisms - such as the N_2O-reducers harbouring *nosZII* that have been characterized to date - to grow in the system. However, under both conditions, a community with high N_2O reducing capacity (*i.e.* marked increase in *nosZ*/*nir*) could not be enriched for, nor could the specific denitrification activity be completely washed out. The ratio of abundance *nosZ/nir* obtained was similar to the one in (Conthe, Wittorf, Kuenen, Kleerebezem, Hallin, et al. 2018), where a shorter SRT was imposed (1.5 d). Therefore, either *(i)* the imposed SRT was still not enough to allow for the growth of specialist N_2O-reducers or *(ii)* the ecophisyological reasons behind the selection for these bacteria in nature are more complex than growth rate and substrate affinity (defined as μ_{max}/K_s) alone.

Nevertheless, cultivation under N_2O limitation did result in a 12 orders of magnitude increase in the relative abundance of *nosZII* (often associated with specialists), as well as in a 4 orders of magnitude lower *nosZI* and *nirS* (usually generalist) relative abundances than under acetate limitation. Yet, *nirK* was present in comparable levels in both systems, and *nir* dominated over *nosZ (50:1)* under N_2O limitation. Thus, affinity for N_2O at the imposed SRT was not the driving selecting factor.

Conversely, and contrary to our expectations, under acetate limitation *nosZ* dominated over *nir* (5:1). Cultivation with excess N_2O was shown to negatively affect cellular metabolism, as supported by lower biomass yields (Y_{XAc}, Y_{XN2O}) and higher maintenance coefficient than the ones obtained under N_2O limitation. Therefore, we hypothesize that N_2O reductase encoding genes (*nosZ*) were present in higher abundance than *nir* under N_2O excess possibly for detoxification purposes.

Ultimately, consistent PHA accumulation was observed both under acetate and N_2O limiting conditions, and two different mechanisms are proposed. Under acetate limitation, inactivation of methionine synthase by excess N_2O limits the flux of carbon to biomass. Consequently, PHB is synthesized in order to avoid acetyl-CoA accumulation. Under N_2O limitation, the lack of electron acceptor prevents ATP synthesis. In this case, PHB synthesis could limit the accumulation of NADH and acetyl-CoA.

5. RECOMMENDATIONS

I. Soils allow for the formation of biofilms and are the ecosystems were high *nosZ* clade II abundances have been found (Jones, Spor, Brennan, Breuil, Bru, Lemanceau, Griffiths, et al. 2014). Thus, a biofilm reactor might be the most suitable one to select for specialist N_2O-reducers.

II. We hypothesize that the dominance of *nosZ* over *nir* under N_2O excess is related to a detoxification mechanism. In order to prove this, studying the effect of a step-wise increase or decrease in the N_2O gas flow on the PHA content is highly recommendable. Moreover, in order to verify whether methionine synthase is inactivated by N_2O, an analysis of the proteome of the cells exposed to different N_2O concentrations would be of great interest.

III. Studies targeting different and more complex substrates are required to elucidate the impact of using acetate as sole carbon source on the selection mechanisms.

IV. In both reactors, while fluctuations in denitrifying activities were experienced, the relative abundance of *nir* remained fairly constant. The use of combined meta-transcriptomic and meta-proteomic approaches could provide further details on the transcriptional or translational regulation of this gene.

V. The hypothesis explaining the accumulation of PHA were based on *(i)* acetate diffusing passively to the cell and *(ii)* a NADH-dependent PHB synthesis. For the first one, repeating the experiment at lower pH is recommended. In this situation, the concentration of the protonated form of acetate, the one able to diffuse passively into the cell, will increase. Thus, an increase in the PHA content is expected. For the second one, enzymatic assays to check if this pathway is present in the microbial community are required, and currently being performed.

VI. Last, the production of hydroxymethylfurfural (HMF) during the fermentation of PHA has remains poorly understood. Thus, an analysis of the metabolic pathways that could produce it and its role in the fermentation is needed.

6. REFERENCES

Amos, D A, and Michael J Mclnerney. 1993. “Hicmbiology by an Acetoacetyl-Coenzyme A Reductase in Syntrophomonas Wolfei.” *Archives of Microbiology* 159: 16–20.

Beun, J J, K Dircks, M C M Van Loosdrecht, and J J Heijnen. 2002. “Polyhydroxybutyrate Metabolism in Dynamically Fed Mixed Microbial Cultures.” *Water Research* 36: 1167–80.

Beun, J J, E V Verhoef, M C M Van Loosdrecht, and J J Heijnen. 2000. “Stoichiometry and Kinetics of Poly-b -Hydroxybutyrate Metabolism Under Denitrifying Conditions in Activated Sludge Cultures.” *Biotechnology and Bioingeneering* 68(5): 496–507.

Braker, Gesche, and Ralf Conrad. 2011. “Diversity, Structure, and Size of N_2O-Producing Microbial Communities in Soils—What Matters for Their Functioning?” *Advances in Applied Microbiology* 75: 33–70.

Brigham, Christopher J, Kazuhiko Kurosawa, Chokyun Rha, and Anthony J Sinskey. 2011. “Bacterial Carbon Storage to Value Added Products.” *Microbial & Biochemical Technology*.

Casal, Margarida, Helena Cardoso, and Cecilia Le. 1996. “Mechanisms Regulating the Transport of Acetic Acid in Saccharomyces Cerevisiae.” *Microbiology* 142: 1385–90.

Cavaillé, Laëtitia, Maria Albuquerque, Estelle Grousseau, and Anne-sophie Lepeuple. 2016. “Bioresource Technology Understanding of Polyhydroxybutyrate Production under Carbon and Phosphorus-Limited Growth Conditions in Non-Axenic Continuous Culture.” *Bioresource Technology* 201: 65–73.

Chen, Jinzhu et al. 2014. “Conversion of Fructose into 5-Hydroxymethylfurfural Catalyzed by Recyclable Sulfonic Acid-Functionalized Metal–organic Frameworks.” *Green Chemistry* 16: 2490–99.

Conthe, Monica, Lea Wittorf, J. Gijs Kuenen, Robbert Kleerebezem, Sara Hallin, et al. 2018. “Growth Yield and Selection of NosZ Clade II Types in a Continuous Enrichment Culture of N_2O Respiring Bacteria.” *Environmental Microbiology Reports* 10(3): 239–44.

Conthe, Monica, Lea Wittorf, J. Gijs Kuenen, Robbert Kleerebezem, Mark C.M. Van Loosdrecht, et al. 2018. “Life on N_2O: Deciphering the Ecophysiology of N_2O Respiring Bacterial Communities in a Continuous Culture.” *ISME Journal* 12(4): 1142–53. http://dx.doi.org/10.1038/s41396-018-0063-7.

Conthe, Monica, Camiel Parchen, et al. 2018. “O_2 versus N_2O Respiration in a Continuous Microbial Enrichment.” *Applied Microbiology and Biotechnology*.

Conthe, Monica, J. Gijs Kuenen, Robbert Kleerebezem, and Mark C.M. van Loosdrecht. 2018. “Exploring Microbial N_2O Reduction: A Continuous Enrichment in Nitrogen Free Medium.” *Environmental Microbiology Reports* 10(1): 102–7.

Costa, Engràcia, Julio Pérez, and Jan Ulrich Kreft. 2006. “Why Is Metabolic Labour Divided in Nitrification?” *Trends in Microbiology* 14(5): 213–19.

Dawes, Edwin A. 1988. “Polyhydroxybutyrate : An Intriguing Biopolymer.” *Bioscience Reports* 8(6): 537–47.

Domeignoz-Horta, LA et al. 2015. “The Diversity of the N_2O Reducers Matters for the N_2O:N_2 denitrification End-Product Ratio across an Annual and a Perennial Cropping System.” *Frontiers in Microbiology* 6(SEP).

Domeignoz-Horta, LA et al.. 2016. “Non-Denitrifying Nitrous Oxide-Reducing Bacteria - An Effective N_2O Sink in Soil.” *Soil Biology and Biochemistry* 103: 376–79. http://dx.doi.org/10.1016/j.soilbio.2016.09.010.

Egli, Thomas. 1991. “On Multiple-Nutrient-Limited Growth of Microorganisms , with Special Reference to Dual Limitation by Carbon and Nitrogen Substrates.” *Antonie van Leeuwenhoek* 60(1972): 225–34.

Filipe, Carlos D M, Glen T Daigger, and C P Leslie Grady Jr. 2001. “A Metabolic Model for Acetate Uptake Under Anaerobic Conditions by Glycogen Accumulating Organisms : Stoichiometry , Kinetics , and the Effect of PH.” *Biotechnology and Bioingeneering* 76: 18–31.

Frank, SE. 1999. “Growth Characteristics of Acinetobacter Johnsonii 210A under Single and Dual Nutrient Limitation with Special Reference to Carbon, Nitrogen and Phosphorus.”

Graf, Daniel R H, Christopher M. Jones, and Sara Hallin. 2014. “Intergenomic Comparisons Highlight Modularity of the Denitrification Pathway and Underpin the Importance of Community Structure for N_2O Emissions.” *PLoS ONE* 9(12): 1–20.

Hall, B D, G S Dutton, and J W Elkins. 2007. “The NOAA Nitrous Oxide Standard Scale for Atmospheric Observations.” *Journal of Geophysical Research* 112: 1–9.

Hallin, Sara et al. 2018. “Genomics and Ecology of Novel N_2O-Reducing Microorganisms.” *Trends in Microbiology* 26(1): 43–55.

Han, X, A Aslanian, and JR Yates. 2009. “Mass Spectrometry for Proteomics.” *Current Opinion in Chemical Biology* 12(5): 483–90.

Hansen, D K. 1986. “Effects of Nitrous Oxide on Macromolecular Content and DNA Synthesis in Rat Embryone.” *Survey of Anesthesiology* 238: 985–89.

Hardie, DG. 2015. “AMPK : Positive and Negative Regulation , and Its Role in Whole-Body Energy Homeostasis.” *Current Opinion in Cell Biology* 33: 1–7. http://dx.doi.org/10.1016/j.ceb.2014.09.004.

De Heyder, B, Peter Vanrolleghem, Herman Van Langenhove, and Willy Verstraete. 1997. “Kinetic Characterization of Mass Transfer Limited Biodegradation of a Low Water Soluble Gas in Batch Experiments — Necessity for Multiresponse Fitting.” *Biotechnology and Bioingeneering* 55 (3): 511–19.

Houtkooper, RH, C Canto, RJ Wanders, and J Auwerx. 2010. “The Secret Life of NAD+: An Old Metabolite Controlling New Metabolic Signaling Pathways.” *Endocrinology Reviews*.

Hsu, Juno, and Michael J Prather. 2010. “Global Long - Lived Chemical Modes Excited in a 3 - D Chemistry Transport Model : Stratospheric N 2 O , NO y , O 3 and CH 4 Chemistry.” *Geophysical Research Letters* 37: 1–5.

Huda, S M Shamsul, Hiroyasu Satoh, and Takashi Mino. 2016. “Anaerobic Degradation of Polyhydroxyalkanoate Accumulated in Activated Sludge in the Absence of Anaerobic Digested Sludge.” *Journal of Water and Environmental Technology* 14(4): 236–46.

IPCC. 2014. *Climate Change 2014 Synthesis Report Summary Chapter for Policymakers*.

Ji, Q et al. 2015. “Nitrous Oxide Production by Nitrification and Denitrification in the Eastern Tropical

South Pacific Oxygen Minimum Zone." *Geophysical Research Letters* (2): 755–64.

Johnson, D, Felix Goldschmidt, Elin E. Lilja, and Martin Ackermann. 2012. "Metabolic Specialization and the Assembly of Microbial Communities." *ISME Journal* 6(11): 1985–91. http://dx.doi.org/10.1038/ismej.2012.46.

Johnson, Katja et al. 2009. "Enrichment of a Mixed Bacterial Culture with a High Polyhydroxyalkanoate Storage Capacity." *Biomacromolecules* 10: 670–76.

Jones, Christopher M. et al. 2013. "The Unaccounted yet Abundant Nitrous Oxide-Reducing Microbial Community: A Potential Nitrous Oxide Sink." *ISME Journal* 7(2): 417–26. http://dx.doi.org/10.1038/ismej.2012.125.

Jones, Christopher M., Ayme Spor, Fiona P. Brennan, Marie Christine Breuil, David Bru, Philippe Lemanceau, Bryan Griffiths, et al. 2014. "Recently Identified Microbial Guild Mediates Soil N_2O Sink Capacity." *Nature Climate Change*.

Jones, Christopher M, Ayme Spor, Fiona P Brennan, Marie-christine Breuil, David Bru, Philippe Lemanceau, Bryan Gri, et al. 2014. "Recently Identified Microbial Guild Mediates Soil N 2 O Sink Capacity." *Nature Climate Change* 4(July): 801–5.

Konings, W I L N. 1977. *Active Transport of Solutes in Bacterial Membrane Vesicles*.

Kool, Dorien M et al. 2011. "Soil Biology & Biochemistry Nitri Fi Er Denitri Fi Cation as a Distinct and Signi Fi Cant Source of Nitrous Oxide from Soil." *Soil Biology and Biochemistry* 43: 174–78.

Korkakaki, Emmanouela, Mark C M Van Loosdrecht, and Robbert Kleerebezem. 2017. "Impact of Phosphate Limitation on PHA Production in a Feast-Famine Process." *Water Research* 126: 472–80. https://doi.org/10.1016/j.watres.2017.09.031.

Kuypers, Marcel M.M., Hannah K. Marchant, and Boran Kartal. 2018. "The Microbial Nitrogen-Cycling Network." *Nature Reviews Microbiology* 16(5): 263–76. http://dx.doi.org/10.1038/nrmicro.2018.9.

Larsson, Christer, and Inga-lill Pa. 2000. "The Importance of ATP as a Regulator of Glycolytic Flux in Saccharomyces Cerevisiae." *Yeast* 16: 797–809.

Lehninger, AL, DL Nelson, and MM Cox. 1993. *Principles of Biochemistry*. New York: Worth Publishers.

Ling, Chen et al. 2018. "Engineering NADH / NAD + Ratio in Halomonas Bluephagenesis for Enhanced Production of Polyhydroxyalkanoates (PHA)." *Metabolic Engineering* 49(July): 275–86. https://doi.org/10.1016/j.ymben.2018.09.007.

Lipson, DA, RK Monson, and SK Schmidt. 2009. "The Trade-off between Growth Rate and Yield in Microbial Communities and the Consequences for under-Snow Soil Respiration in a High Elevation Coniferous Forest." *Biogeochemistry*. https://doi.org/10.1007/s10533-008-9252-1.

Liu, Yiwen, Lai Peng, Xueming Chen, and Bing-jie Ni. 2015. "Mathematical Modeling of Nitrous Oxide Production during Denitrifying Phosphorus Removal Process." *Environmental Science & Technology* 49: 8595–8601.

Locasale, JW, and LC Cantley. 2011. "Metabolic Flux and the Regulation of Mammalian Cell Growth." *Cell Metabolism* 14(4): 443–51.

Louca, Stilianos, Michael Doebeli, and Laura Wegener Parfrey. 2018. "Correcting for 16S RRNA Gene Copy Numbers in Microbiome Surveys Remains an Unsolved Problem." *Microbiome* 6(41): 1–12.

Machida, T., T. Nakazawa, and O. Watanabe. 1995. "Increase in the Atmospheric Nitrous Oxide Concentration during the Last 250 Yeards." *Geophysical Research Letters* 22(21): 2921–24.

Metay, Aurélie et al. 2007. "N_2O and CH4 Emissions from Soils under Conventional and No-till Management Practices in GoiâNia (Cerrados,Brazil)." *Geoderma* 141: 78–88.

Miyahara, Yuki, Mino Oota, and Takeharu Tsuge. 2018. "NADPH Supply for Poly (3-Hydroxybutyrate) Synthesis Concomitant with Enzymatic Oxidation of Phosphite." *Journal of Bioscience and Bioengineering* 126(6): 764–68. https://doi.org/10.1016/j.jbiosc.2018.05.026.

Montzka, S. A., E. J. Dlugokencky, and J. H. Butler. 2011. "Non-CO 2 Greenhouse Gases and Climate Change." *Nature* 476(7358): 43–50. http://dx.doi.org/10.1038/nature10322.

Muñoz, Cristina, Leandro Paulino, Carlos Monreal, and Erick Zagal. 2010. "Greenhouse Gas (CO_2 and N_2O) Emissions from Soils: A Review." *Chilean Journal of Agricultural Research* 70(3): 485–97.

Nagele, P et al. 2008. "Influence of Methylenetetrahydrofolate Reductase Gene Polymorphisms on Homocysteine Concentrations after Nitrous Oxide Anesthesia." *Anesthesiology* 109: 36–43.

Orellana, LH et al. 2014. "Detecting Nitrous Oxide Reductase (NosZ) Genes in Soil Metagenomes : Method Development and Implications for The." *mBio* 5(3): 1–8.

Pauleta, Sofia R, Marta S P Carepo, and Isabel Moura. 2019. "Source and Reduction of Nitrous Oxide." *Coordination Chemistry Reviews* 387: 436–49. https://doi.org/10.1016/j.ccr.2019.02.005.

Pfeiffer, Thomas, and Sebastian Bonhoeffer. 2004. "Evolution of Cross-Feeding in Microbial Populations." *The American Naturalist* 163(6): E126–35. http://www.journals.uchicago.edu/doi/10.1086/383593.

Pirt, SJ. 1965. "The Maintenance Energy of Bacteria in Growing Cultures." *Proceedings of Royal Society*: 224–231.

Portmann, R W, J S Daniel, and A R Ravishankara. 2012. "Stratospheric Ozone Depletion Due to Nitrous Oxide : Influences of Other Gases." *Philosophical Transactions of the Royal Society B* 367: 1256–64.

Prather, Michael J et al. 2015. "Journal of Geophysical Research : Atmospheres Oxide Including Its Variability." *Journal of Geophysical Research* 120: 5693–5705.

Ravishankara, A R, John S Daniel, and Robert W Portmann. 2009. "Nitrous Oxide (N 2 O): The Dominant Ozone-Depleting Substance Emitted in the 21st Century." *Science* 326: 2007–10.

Reis, M A M et al. 2003. "Production of Polyhydroxyalkanoates by Mixed Microbial Cultures." *Bioprocess Biosystems Engineering* 25(2003): 377–85.

Roco, Constance A. et al. 2017. "Modularity of Nitrogen-Oxide Reducing Soil Bacteria: Linking Phenotype to Genotype." *Environmental Microbiology* 19(6): 2507–19.

Roels, JA. 1980. "Simple Model for the Energetics of Growth on Substrates with Different Degrees of Reduction." *Biotechnology and Bioingeneering* 22: 33–53.

Saikawa, E et al. 2014. "Global and Regional Emissions Estimates for N 2 O." *Atmospheric Chemistry and Physics* 14: 4617–41.

Salehizadeh, H, and M C M Van Loosdrecht. 2004. "Production of Polyhydroxyalkanoates by Mixed Culture : Recent Trends and Biotechnological Importance." *Biotechnology Advances* 22: 261–79.

Sanford, R. A. et al. 2012. "Unexpected Nondenitrifier Nitrous Oxide Reductase Gene Diversity and Abundance in Soils." *Proceedings of the National Academy of Sciences* 109(48): 19709–14. http://www.pnas.org/cgi/doi/10.1073/pnas.1211238109.

Schreiber, Frank, Pascal Wunderlin, Kai M. Udert, and George F. Wells. 2012. "Nitric Oxide and Nitrous

Oxide Turnover in Natural and Engineered Microbial Communities: Biological Pathways, Chemical Reactions, and Novel Technologies." *Frontiers in Microbiology* 3(OCT): 1–24.

Senior, P J, G A Beech, G A F Ritchiet, and E A Dawes. 1972. "The Role of Oxygen Limitation in the Formation of Poly-P-Hydroxybutyrate during Batch and Continuous Culture of Azotobacter Beijerinckii." *Biochemistry Journal* 31(2): 194–233.

Senior, P J, and Edwin A Dawes. 1973. "A Theoretical Study on the Amount of ATP Required for Synthesis of A." *Biochemistry Journal* 134: 225–38.

Seviour, R J, J G Kuenen, and M S M Jetten. 2000. "Nitrous Oxide (N_2O) Production by Alcaligenes Faecalis during Feast and Famine Regimes." *Water Research* 34(7): 2080–88.

Shi, Lei, and Benjamin P Tu. 2015. "Acetyl-CoA and the Regulation of Metabolism: Mechanisms and Consequencesc Access." *Current Opinion in Cell Biology* 33: 125–31.

Soler-Jofra, Aina et al. 2016. "Importance of Abiotic Hydroxylamine Conversion on Nitrous Oxide Emissions during Nitritation of Reject Water." *Chemical Engineering Journal* 287: 720–26. http://dx.doi.org/10.1016/j.cej.2015.11.073.

Sorokin, Dimitry Y, and Æ Horia Banciu. 2003. "Growth Physiology and Competitive Interaction of Obligately Chemolithoautotrophic , Haloalkaliphilic , Sulfur-Oxidizing Bacteria from Soda Lakes." *Extremophiles* 7: 195–203.

Steinbiichel, A. 1992. "Cloning and Nucleotide Sequences of Genes Relevant for Biosynthesis of Poly(3-Hydroxybutyric Acid) In." *European Journal of Biochemistry* 150: 135–50.

Steinbiichel, Alexander. 1991. "3 Polyhydroxyalkanoic Acids." In *Biomaterials: Novel Materials from Biological Sources*, , 123–213.

Stouthamer, AH. 1973. "A Theoretical Study on the Amount of ATP Required for Synthesis of Macrobial Cell Material." *Antonie van Leeuwenhoek* 39: 545–65.

Taylor, R T. 1982. "B12-Dependent Methionine Biosynthesis." *Biochemistry and Medicie* 2: 307–55.

Third, Katie A, Mark Newland, and Ralf Cord-ruwisch. 2003. "The Effect of Dissolved Oxygen on PHB Accumulation in Activated Sludge Cultures." *Biotechnology and Bioingeneering* 82(2): 238–50.

Thomson, Andrew J et al. 2012. "Biological Sources and Sinks of Nitrous Oxide and Strategies to Mitigate Emissions." *Philosophical Transactions of the Royal Society B* 367: 1157–68.

Tilman, David, Christian Balzer, Jason Hill, and Belinda L Befort. 2011. "Global Food Demand and the Sustainable Intensi Fi Cation of Agriculture." *Proceedings of the National Academy of Sciences* 108(50): 20260–64.

Velasco, M, A Wahl, and MCM van Loosdrecht. 2019. "Microbial Synthesis of Polyhydroxybutyrate: A Thermodynamic Study of Different Synthesis Routes." *Unpublished work*.

Veraart, AJ et al. 2017. "Abundance , Activity and Community Structure of Denitrifiers in Drainage Ditches in Relation to Sediment Characteristics , Vegetation And." *Ecosystems* 20: 928–43.

Vishniac, W, and M Santer. 1957. "The Thiobacili." *Microbiology and Molecular Biology Review*: 195–213.

Ward, C, and Hull Hu. 1977. "Effect of Oxygen and Nitrogen Limitation on Poly-p-Hydroxybutyrate Biosynthesis in Ammonium-Grown Azo to Bac Ter Beijerinckii." *Journal of General Microbiology* 102(May): 61–68.

Weimann, J. 2003. "Toxicity of Nitrous Oxide." *Best Practice & Research* 17(1): 47–61.

Weiss, RF. 1980. “NItrous Oxide Solubility in Water and Seawater.” *Marine Chemistry* 8: 347–59.

Wen, Qinxue, Zhiqiang Chen, Ting Tian, and Wei Chen. 2010. “Effects of Phosphorus and Nitrogen Limitation on PHA Production in Activated Sludge.” *Journal of Environmental Sciences* 22(10): 1602–7. http://dx.doi.org/10.1016/S1001-0742(09)60295-3.

Wrage, N, G L Velthof, M L Van Beusichem, and O Oenema. 2001. “Role of Nitrifier Denitrification in the Production of Nitrous Oxide.” *Soil Biology and Biochemistry* 33: 1723–32.

Yanai, Yosuke et al. 2011. “Accumulation of Nitrous Oxide and Depletion of Oxygen in Seasonally Frozen Soils in Northern Japan – Snow Cover Manipulation Experiments.” *Soil Biology and Biochemistry* 43(9): 1779–86.

Yoon, Sukhwan et al. 2016. “Clade I NosZ from Those Harboring Clade II NosZ.” *Applied and Environmetal Microbiology* 82(13): 3793–3800.

Zhao, Shun et al. 2011. “One Pot Production of 5-Hydroxymethylfurfural with High Yield from Cellulose by a Brønsted – Lewis – Surfactant-Combined Heteropolyacid Catalyst W.” *Chemical Communications* 47: 2176–78.

Zumft, W. G. 1997. “Cell Biology and Molecular Basis of Denitrification,.” *Microbiology and Molecular Biology Review* 61(4): 533–616.

7. APPENDIX

7.1. K_La determination

The affinity for N_2O is expected to be a selecting factor for non-denitrifying N_2O-reducers. Therefore, ensuring that this is the limiting substrate is essential for the chemostat experiments. Given the high solubility of N_2O in water (Weiss 1980), assuming that the concentration of this gas in the gas and liquid phase are in equilibrium is reasonable. Shall it be the case, its concentration in the reactor can be calculated with an off-gas analyser, reducing the complexity of the experiments. To strength the validity of this assumption, the volumetric gas-liquid (G-L) mass transfer coefficient of the reactor for N_2O (k_La_{N2O}) was calculated.

Among all the different methods, the dynamic one (also known as gas in – gas out) has been chosen due to its simplicity. It consists of saturating the liquid in the reactor with a gas (N_2, for instance) and then saturating it again with the gas of interest (N_2O), measuring its concentration in the liquid. Because the equipment required to calculate the concentration of N_2O in the liquid was not available, the experiment has been carried out using air as the second gas, and the concentration of oxygen has been followed.

The dynamics of the mass transfer follow the following equation:

$$\frac{dC}{dt} = k_L a\ (C^* - C) \tag{2}$$

Where *C* stands for concentration in the liquid of the compound of interest, *t* is time, *C** the maximum concentration of the compound in the liquid, based on its concentration in the gas and the Henry coefficient, and k_La the volumetric gas-liquid mass transfer coefficient, a convoluted term that includes the mass transfer coefficient (k_L) and the interfacial area available for mass transfer.

The integration of this equation from time $t_o = 0$ to *t* and concentration $C_0 = 0$ to C* gives:

$$C = C^*(1 - e^{-k_L a t}) \tag{3}$$

To which the experimental results can be fitted with a non-linear regression. In this case ,the solver *lqscurvefit* in *MATLAB* was used. Finally, the k_La_{N2O} can be obtained using equation (4), which related the k_La of two different components taking into account their diffusion coefficients and is valid for low soluble components and a liquid interphase in turbulent motion (De Heyder et al. 1997).

$$k_L a_{N_2O} = \frac{k_L a_X}{\sqrt{D_x / D_{N_2O}}} \quad (4)$$

The obtained $K_L a_{N2O}$ values can be seen in Table S 1. The experimental oxygen concentration and the fitting with the calculated $k_L a$ is shown in Figure S 1.

Table S 1. kLa_{O2} values obtained using oxygen in air with the dynamic method and transformed to kLa_{N2O} with equation 4.

Total flow [mL·min^{-1}]	100	150	200
$K_L a_{N2O}$ [h^{-1}]	15.91	21.26	25.57

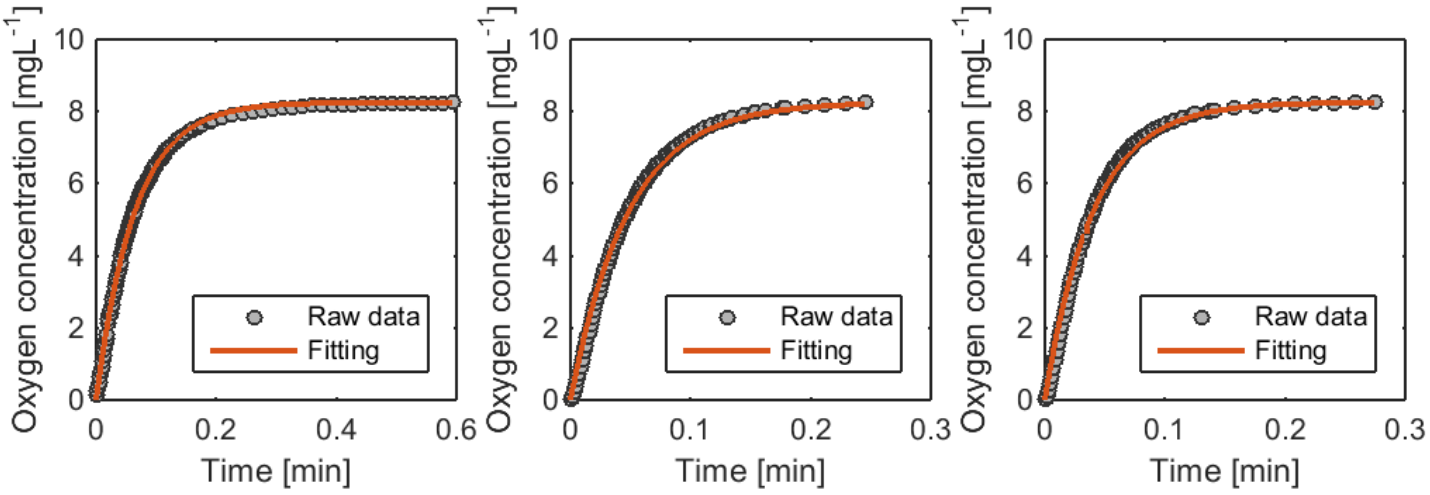

Figure S 1. Change in the oxygen concentration along time (grey dots) and the calculated ones with the values obtained with the non-linear correlation (red line).

7.2. qPCR and amplicon sequencing

The primers and recipes for qPCR and amplicon can be found in the following table.

Table S 2. Primers and recipes used for qPCR and amplicon sequencing

Genes Primer names	Sequence (5'-3')	References	Thermal cycling	Efficiency (qPCR) (%)
16S rRNA				
341F	CCT ACG GGA GGC AGC AG	López-Gutiérrez *et al.* 2004	(95 ºC, 7 min) x 1	95
534R	ATT ACC GCG GCT GCT GGC A		(95°C, 15 s; 60°C, 30 s; 72°C, 30 s; 80°C, 5 s) x 35	
nirK			(95 ºC, 7 min) x 1	
876F	ATYGGCGGVCAYGGCGA	Henry *et al.,* 2004	(95°C, 15 s;(63°C – 58°C, -1°/cycle), 30 s; 72°C, 30 s) x 6	85
R3Cu	GCCTCGATCAGRTTGTGGTT	Hallin and Lindgren, 1999	(95°C, 15 s; 58°C, 30 s; 72°C, 30 s; 80°C, 5 s) x 35	
nirS			(95 ºC, 7 min) x 1	
cd3aFm	AACGYSAAGGARACSGG	Throbäck et al., 2004	(95°C, 15 s;(65°C – 60°C, -1°/cycle), 30 s; 72°C, 30 s) x 6	93
R3cdm	GASTTCGGRTGSGTCTTSAYGAA		(95°C, 15 s; 58°C, 30 s; 72°C, 30 s; 80°C, 5 s) x 35	
nosZI			(95 ºC, 7 min) x 1	
1840F	CGC RAC GGC AAS AAG GTS MSS GT	Henry et al., 2004	(95°C, 15 s;(65°C – 60°C, -1°/cycle), 30 s; 72°C, 30 s) x 6	97
2090R	CAK RTG CAK SGC RTG GCA GAA		(95°C, 15 s; 58°C, 30 s; 72°C, 30 s; 80°C, 5 s) x 35	
nosZII				
nosZII-F	CTI GGI CCI YTK CAY AC	Jones *et al.,* 2013	(95 ºC, 7 min) x 1	86
nosZII-R	GCI GAR CAR AAI TCB GTR C		(95°C, 15 s; 54°C, 30 s; 72°C, 30 s; 80°C, 5 s) x 40	
16S rRNA (sequencing)		Takahashi et al., 2014		
Pro341F	CCTACGGGNBGCASCAG			
Pro805R	GACTACNVGGGTATCTAATCC			

7.3. Maintenance coefficient determination

Maintenance is defined as *the energy consumed for functions other than the production of new cell material* [36]. Therefore, the maintenance coefficient could be determined by maintaining the culture at non-growth conditions and observing the amount of substrate consumed. Another approach is to grow the microbial communities at different growth rates in order to elucidate the maintenance coefficient with a linear regression. The later was the chosen method, which goes as follows:

The substrate consumed is used either for growth or maintenance:

Consumed substrate	=	Growth	+	Maintenance
$\frac{dC_s}{dt}$	=	$\left(\frac{dC_s}{dt}\right)_G$	+	$\left(\frac{dC_s}{dt}\right)_M$

Where C_s stand for substrate concentration and t is time. It can also be written as:

$$Y_{\frac{s}{x}} \cdot \mu \cdot C_x = \left(Y_{\frac{s}{x}}\right)_G \cdot \mu \cdot C_x + m \cdot C_x$$

With μ representing the growth rate, $Y_{w/z}$ the yield of w on z, C_x the biomass concentration and m the maintenance coefficient. Dividing by μC_x:

$$Y_{\frac{s}{x}} = \left(Y_{\frac{s}{x}}\right)_G + \frac{m}{\mu}$$

With the data obtained in this work and retrieved from (Conthe, Wittorf, Kuenen, Kleerebezem, Van Loosdrecht, et al. 2018), the following plots and maintenance coefficients were obtained:

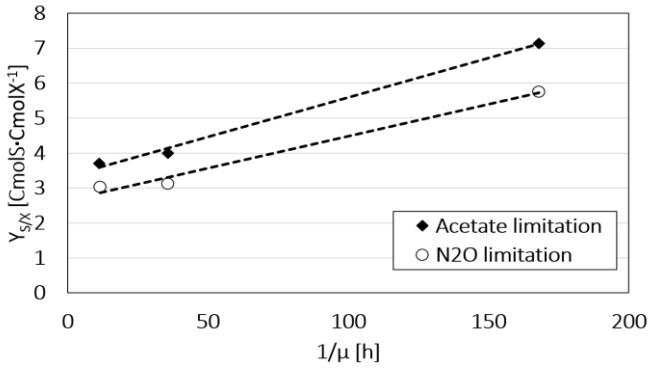

Figure S 2. Correlation between the biomass yield on acetate and the growth rate under acetate or N_2O limitation. Data obtained from this work and (Conthe, Wittorf, Kuenen, Kleerebezem, Van Loosdrecht, et al. 2018)

7.4. Microscope images of cells with PHA

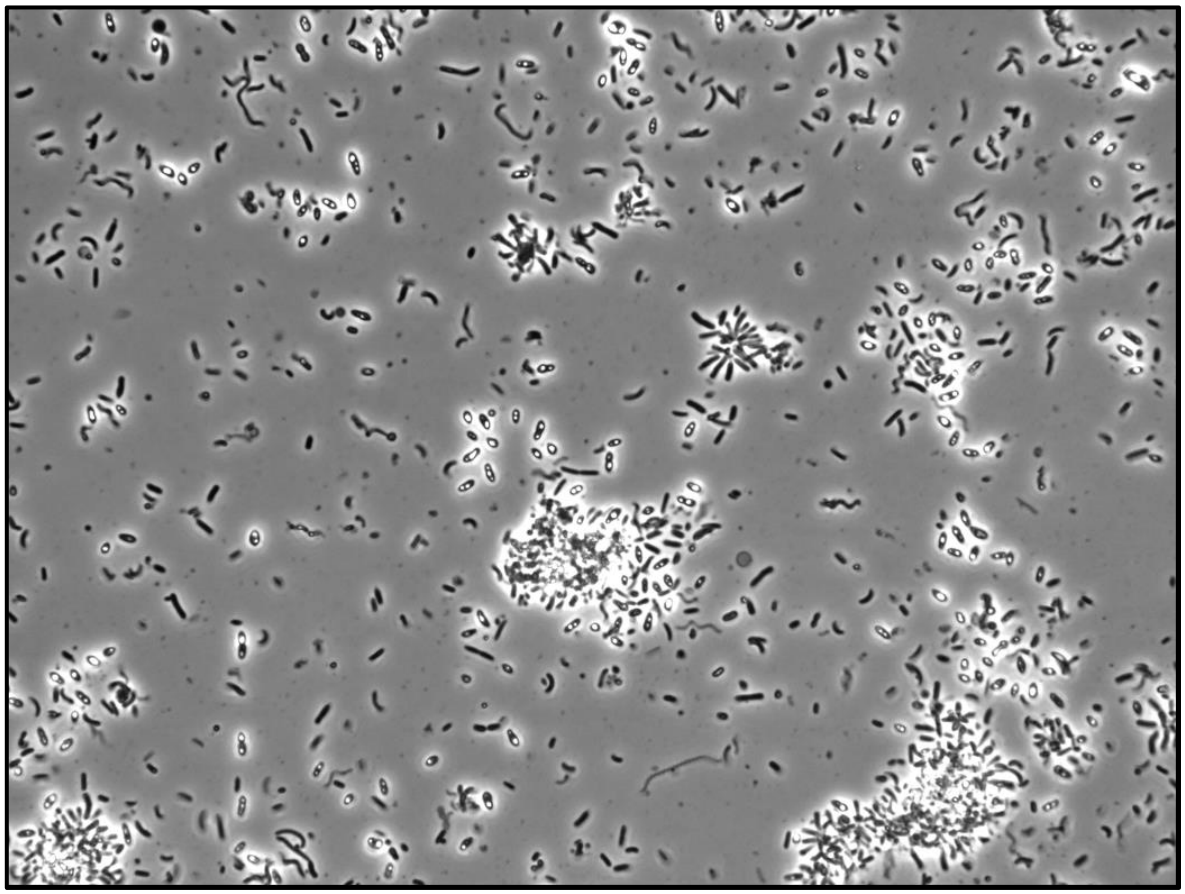

Figure S 3. Microscope image of the cells in R_1 taken on day -30 from R_1.Multiple cells contain shiny granules of PHA.

7.5. Batch test with PHA

Batch test were run to monitor the denitrification capacity of the microbial communities in each reactor as described in Section 2.2. A representative example of each of the three conditions tested is shown in Figure S 4. As expected, acetate was consumed after it was added (t = 16.5 h) with N_2O in the tested conditions (top), and remained constant in the controls with dead biomass (bottom). However, quantifiable concentrations of acetate were found after overnight cultivation of the controls with alive biomass (center), where acetate was not added. As proved during the PHA fermentation experiment (Section 0), acetate release is a consequence of the fermentation of PHA under anaerobic conditions. The fact that this compound is detected in the base case (top) before it was manually injected (t = 16.5h) supports this theory. On top of that, no acetate was found before its injection in the control with dead biomass (at t = 16h), underlining the fact that acetate release is a consequence of a cellular activity and not an artefact of the experiment.

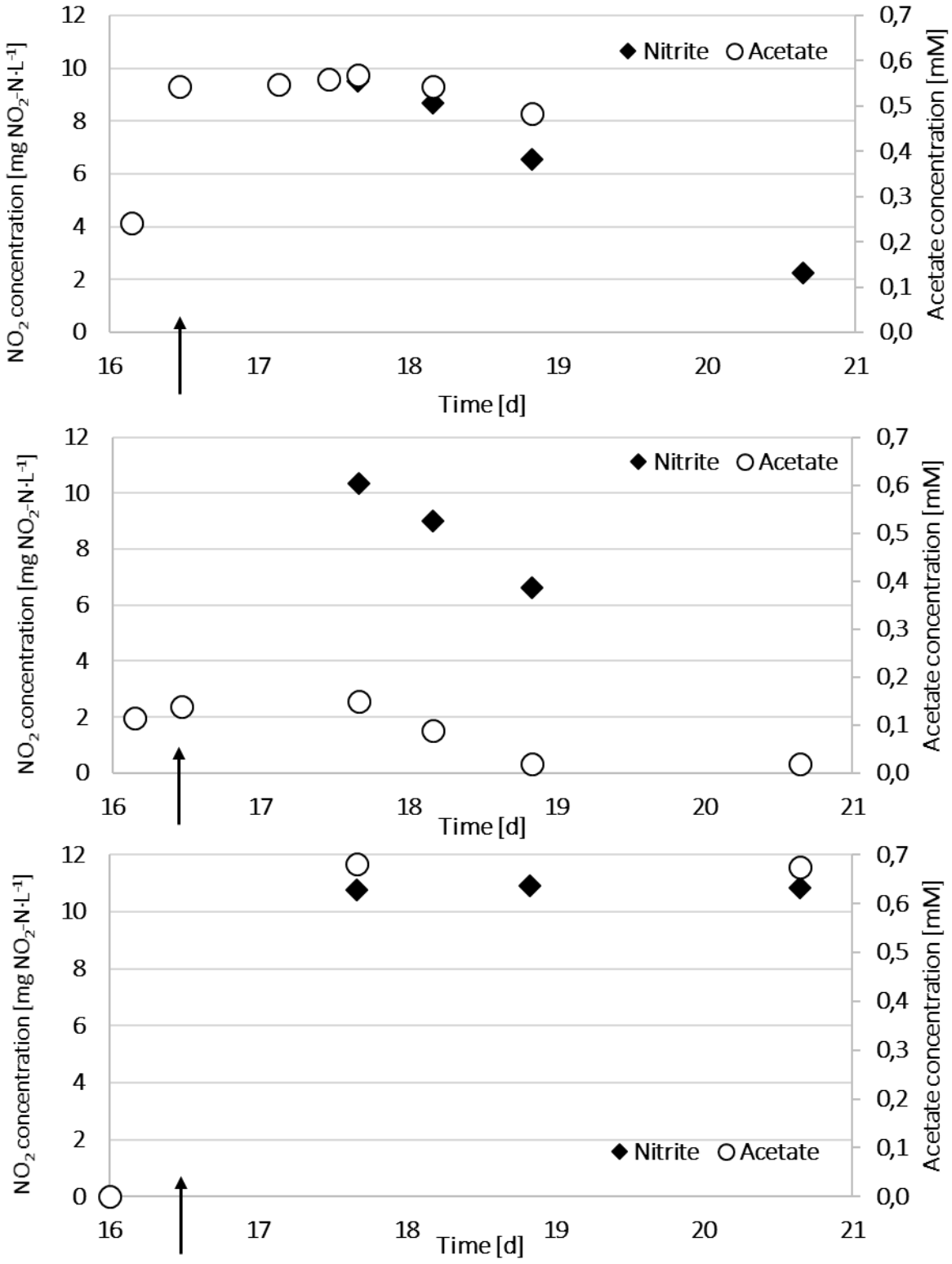

Figure S 4. Evolution of the nitrite (NO2) and acetate concentrations during the batch tests. In all cases the flasks were inoculated and flushed with N2 to induce the anaerobic conditions at time 0, when no nitrite nor acetate are present. ***Top.*** *Acetate oxidation is coupled to nitrite reduction. Intriguingly, acetate is already present at t = 16h, before the acetate is spiked (t = 16.5 h).* ***Center****. Same conditions as in the first flask, but no acetate is spiked. However, acetate is found again. In both cases the production of this compound was attributed to the fermentation of PHA.* ***Bottom****. Similar conditions to the first case, but with autoclaved biomass. In this case, no acetate was detected before it is manually injected, supporting the hypothesis that the presence of acetate is due to cellular activity. ♦ Nitrite , O Acetate ↑ Acetate injection.*

7.6. Reactor data: acetate, ammonia, biomass and gas composition

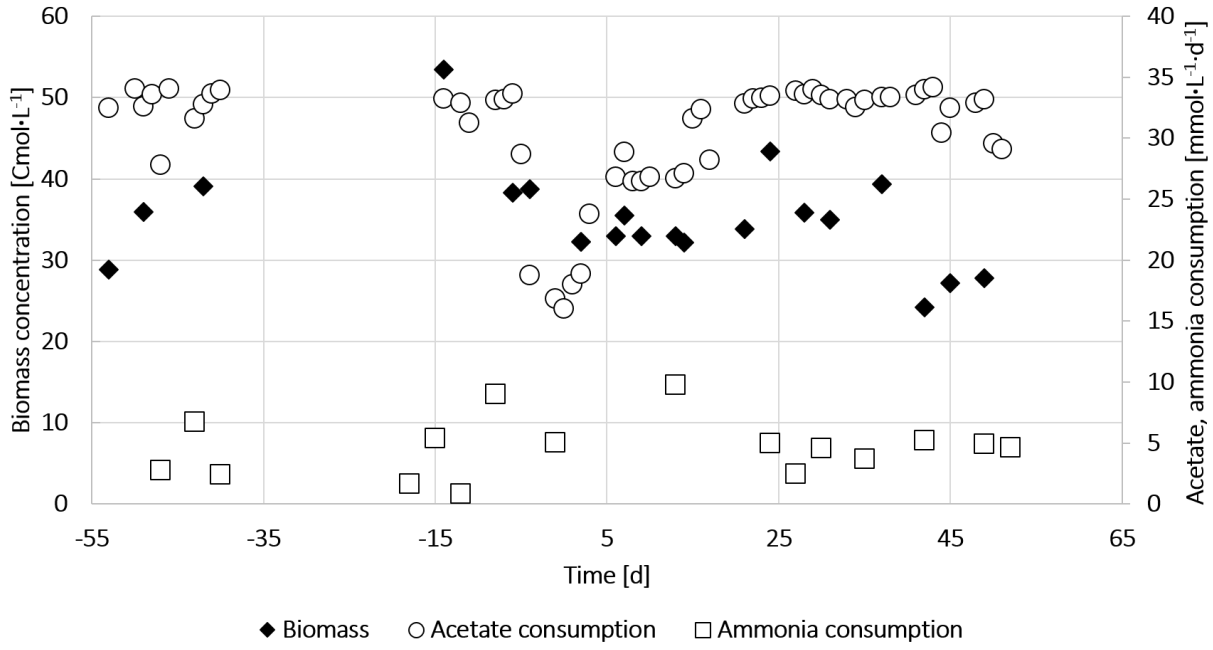

Figure S 5. Biomass concentration and acetate and ammonia in R_1, under acetate-limiting conditions.

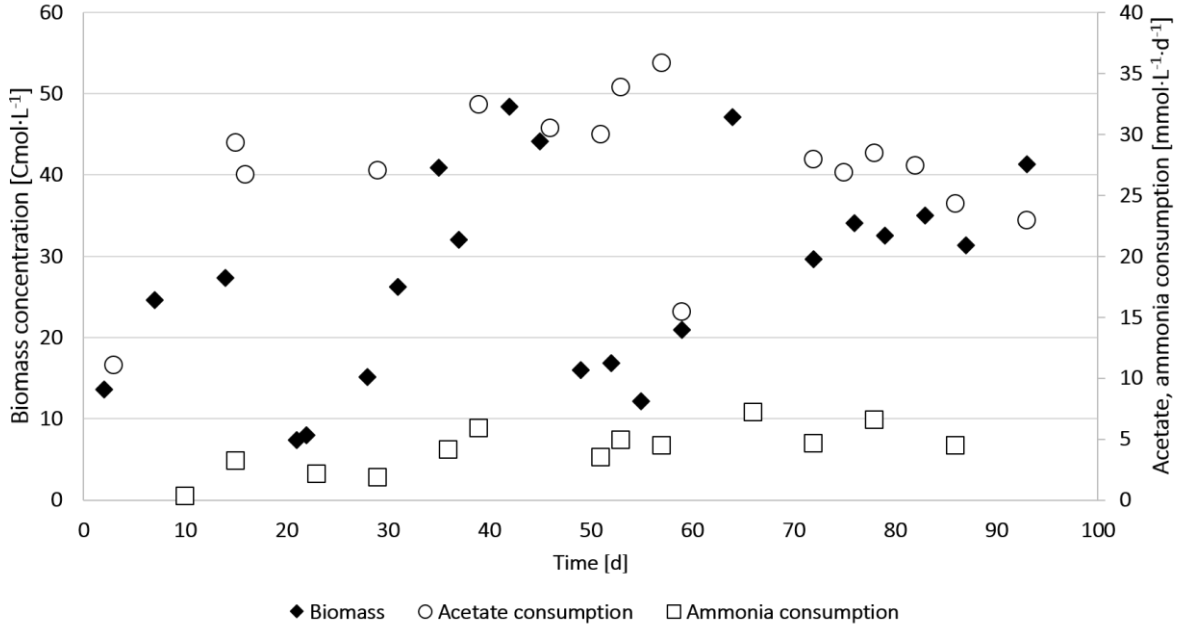

Figure S 6. Biomass concentration and acetate and ammonia in R_2, under N_2O-limiting conditions.

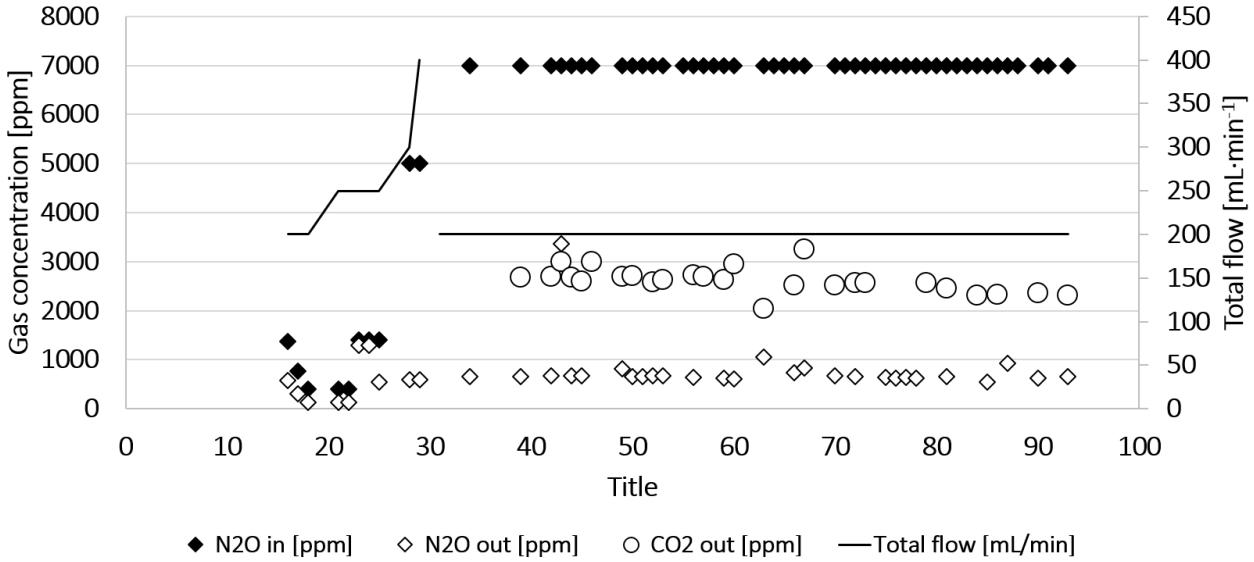

Figure S 7. N_2O and CO_2 concentrations in the inlet and off gas of R_2. Total flow in is also represented.

7.7. Electrophoresis geles

The standard curve for the absolute quantification of the gen abundance in the reactors was done with the PCR products of the samples from day 55. A gel electrophoresis was done to check the purity of the samples. All the products were pure but the one of nirK. This correlates with nirK having the lowest efficiency in the qPCR.

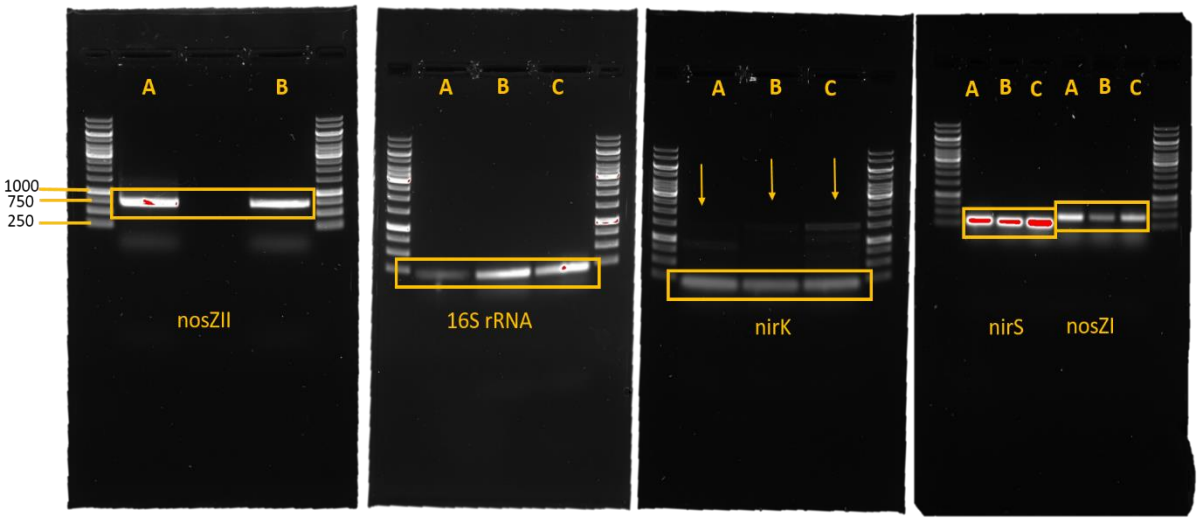

Figure S 8. Electrophoresis geles run to check the purity of the PCR products used to generate the standard curve for the absolute quantification of the functional genes. All genes weee pure, and its band length corresponded to the desired one. Only in the nirK samples other PCR products were found, which explains why the qPCR efficiency for this gen was low. Samples A, B and C correspond to samples taken from R_1 on days 2, 24 and 35 respectively.